WILEY

Research Article

Propagation-Based Train Rescheduling under Recoverable Delay Disturbances

Jun Zhang [ID],[1] **Shuyao Wu** [ID],[1] **Shejun Deng** [ID],[1] **and Yuling Ye** [ID][2]

[1]*Department of Transportation Engineering, College of Architecture Science and Engineering, Yangzhou University, West Huayang Road 196, Jiangsu 225127, China*
[2]*College of Transportation Engineering, Tongji University, Cao'an Highway 4800, Shanghai 201804, China*

Correspondence should be addressed to Jun Zhang; zhangjun93@yzu.edu.cn

Real-time train rescheduling for high-speed railway (HSR) is a pivotal technique in HSR transportation to efficiently recover train operation under disturbance scenarios. This paper aims to put forward an integrated resolving and rescheduling method considering network delay propagation. A tree-based conflict resolution mechanism is first established, with delicate considerations on the strategy's adaptability under different conflict scenarios. By inputting the scheduled arrival and departure time under different conflict resolution strategies, the timetable optimizing model aims to look for an optimal solution with minimal weighted train delay and average train adjustments under necessary technical and empirical constraints solved by a combined algorithm of Pareto optimality and Nash equilibrium, where the feasible solution space is narrowed in advance by a depth-first pruning algorithm. The performance of this coordinated train rescheduling approach is validated by a typical section disturbance in a regional HSR network administrated by the Shanghai Bureau. The results show that the proposed method can well utilizes timetable buffers and organizes train avoidance. The delay propagation characteristics are also simultaneously estimated based on the indicators of cumulative delay and instantaneous delay, which are established considering the spatio-temporal difference between the scheduled and planned timetables, in order to verify the coordination between resolution strategies and train running delays.

1. Introduction

Under the network transportation of high-speed railway (HSR), disturbances of abnormal events are prone to generate train delays and conflicts, which would reduce the railway operation reliability. Therefore, train rescheduling has become the priority of daily train dispatching work, and the corresponding issues such as safety and punctuality are big challenges in the field of HSR dispatching. Faced with complicated and various daily disturbances and transportation scenarios, it is of significant meaning to study the method and theory of train rescheduling for the sake of enhancing the proactivity of dispatching decisions and realizing the smart rescheduling management of HSR. Currently, the daily train dispatching under disturbances is dominated by phased empirical and normative decisions, which cannot guarantee global optimality. Since some major disturbances or breakdowns are difficult to recover without cancelling trains or generating large-scale delays, it is considered recoverable in this paper when a disturbance causes a primary delay less than 40 min on the section with a service frequency lower than 11 trains per hour, depending on the historical dispatching data records of more than 1400 disturbances.

Recently, a great many scholars have made efforts to improve train dispatching and rescheduling under abnormal disturbances. The state of the art is reviewed from the perspectives of conflict resolution, delay management, and timetable rescheduling.

1.1. Conflict Resolution. Conflicts will happen when two or more trains request the same track or block resource simultaneously, which means a train will not release the current occupied resource until it finds an available successive resource. Therefore, the conflict resolution can be seen as a job-shop scheduling problem [1, 2]. Based on this, Mazzarello and Ottaviani [3] built a CDR model using the alternative graph formulation during real-time scheduling, while Toletti et al. [4] devised a resource conflict graph (RCG) model in a similar way, represented by linear constraints including time compatibility and operations consistency.

Under the delay scenario of HSR, the EMU heterogeneity is prone to increase train delay and reduce line capacity; therefore, the resolution of train conflicts should consider the differences in maximum speed, operation priority, and dynamic performance. In order to solve the intertrain conflicts, Corman et al. [5] compared the influence on train delay and energy consumption under WIC (wait in corridors) and GW (green wave) strategies, and Van Thielen et al. [6, 7] proposed a closed-loop conflict prevention strategy based on detecting, preventing, dispatching, and simulating, where the preventing module is comprised of station rerouting and heuristic retiming.

1.2. Delay Management. Generally, train delays are classified into primary delays (initial delays) and secondary delays (consecutive delays). Research methods on railway delay management can be generally divided into regression methods and analytical methods.

The regression-based studies are data-driven models by which train delays can be predicted using technologies such as machine learning and soft computing. Jiang et al. [8] performed a fitting analysis between punctuality and scenario characteristics for primary deviation over 5 minutes. Taking the operation features of section and station as basic inputs, Gao et al. [9] proposed a two-stage delay prediction model through the CART (classification and regression tree) algorithm, where stage 1 calculates the cumulative buffer time of delayed trains and stage 2 predicts the recovery time of primary delay. Similarly, Marković et al. [10] preferred to use SVR (support vector regression) to dynamically describe the relationship between train delay and traffic elements. Huang et al. [11] classified HSR disruptions into four categories according to the scenario attributes and timetable characteristics and found fitted models to estimate affected train number through the Kolmogorov–Smirnov test. In order to predict the recovery time and possible train delays under interlocking system failures, Thaduri [12] established nowcasting models using the nonhomogenous Poisson process and the parametric growth curve. Grandhi et al. [13] analyzed the relationship between parameters of total delay and duration, variables of headway, occurrence time, meteorological environment, and network structure and built a parameter estimation model based on variable importance.

The analytical methods are usually event-driven models, where train delays are calculated upon the interactive operation among trains, stations, and lines. Goverde and Hansen [14, 15] found that the primary delay would cause a domino effect in highly interconnected rail transportation and proposed a max-plus recursion model to analyze the spatio-temporal propagation over a periodic timetable. Given the structural parameters, including timetable supplement, train sequence, and service frequency, Harrod et al. [16] proposed a closed-form analytical model where the cumulative delay is formulated as a polynomial function within the boundaries of the recovery region. Meanwhile, a number of event-based simulation models are introduced to reschedule trains and output delays, including representative models such as job-shop scheduling, discrete event dynamic system (DEDS), and Petri nets [17–19].

Apart from the foregoing studies on delay prediction and analysis, delay propagation has been gradually integrated into the train dispatching and rescheduling problem. By discretizing the spatiotemporal usage of station tracks, Zhang et al. [20] proposed a reoptimization model for train platforming under unexpected train delays, aiming at the comprehensive minimization of train arrival and departure delays and platform track assignment costs. Zhang et al. [21] further considered the equilibrium and volatility of track use during rescheduling formulation, where a higher equilibrium means a higher utilization of track resources and a higher volatility corresponds to a bigger deviation from the original plan. By setting a delay-propagation network, Caprara et al. [22] assigned the arrival path, stopping platform, and departure path for train platforming, with a specific consideration of pattern compatibility. Based on the requirements of minimum safe headway, Feng et al. [23] discussed the calculation model for delay propagation considering front train delay and random interference and revealed the general propagation mechanism through numerical simulations.

1.3. Timetable Rescheduling. Train rescheduling is always a hot topic in the field of railway operation management, including the train timetabling problem (TTP), train platforming problem (TPP), train routing problem (TRP), multitrain trajectory optimization (MTTO) and etc., which can be solved by integer programming or dynamic programming. Table 1 has listed some representative references about timetable rescheduling, where the objectives under different modeling include train delays, affected trains, rolling stock circulation, energy saving, and travel experience, and the applicable scenarios differ in track conditions and disturbance severity (determined by the primary delay, PD). In cases of the partial or complete blockage, Louwerse and Huisman [33] presented integer programming formulations based on the theory of the event-activity network [34], considering the trade-off between cancelling trains and delaying trains. Zhu and Goverde [35] validated that flexible stopping and routing strategies are preferable under high operation frequencies using mixed integer programming (MIP) and gave an emphasis on the dynamic calibration of passenger-dependent weight.

As previously discussed, extensive research has been conducted on the topic of train rescheduling under disturbances. In the studies of train conflict resolution, effective detection methods and resolution strategies have been put

Table 1: Current models on railway timetable rescheduling.

Ref	Model	Problem	Objective	Algorithm	Scenario
Filcek et al. [24]	MILP + LP	TTP	(i) Total cost of delays (ii) Total time of delays	Multilevel heuristic	(i) Double track (ii) Major disturbance (iii) $50 \leq PD \leq 120$ min
Schön and König [25]	SDP	TTP	(i) Total passenger-weighted delay	SDP backward recursion	(i) Single track (ii) Minor disturbance $PD \leq 10$ min
Samà et al. [26]	MIP	TTP TRP	(i) Maximum consecutive delay	Branch and bound tabu search	(i) Medium to major disturbance $15 \leq APD \leq 45$ min
Keita et al. [27]	MIP	TTP	(i) Total weighted delays	Three-step benders decomposition	(i) Multi track (ii) Minor disturbance $5 \leq PD \leq 15$ min
Josyula et al. [28]	MIP	TTP	(i) Total final delay	Depth-first search	(i) Multi track (ii) Minor to medium disturbance $5 \leq PD \leq 25$ min
Zhou et al. [29]	IP	TTP TPP	(i) Total delay (ii) Number of affected trains	Harmony search	(i) Double track (ii) Minor disturbance $2 \leq PD \leq 10$ min
Cavone et al. [30]	MILP	TTP	(i) Passengers' discomfort	Branch and cut	(i) Double track (ii) Minor to medium disturbance $PD \leq 30$ min
Wang and Goverde [31]	DP	TTP MTTO	(i) Energy consumption (ii) Train delays	Driving strategy selection	(i) Single track (ii) Minor disturbance $3 \leq PD \leq 15$ min
Liu et al. [32]	MIP	TTP	(i) Train delays	Simulation + optimization	(i) Double track (ii) Major disturbance $30 \leq PD \leq 60$ min

forward according to the definition and formation of different train conflicts, while the adaptability and optimality of global strategies need further discussion considering the delay propagation effect. Studies in the field of delay management majorly focus on the prediction of train arrival and departure delays, as well as the propagation characteristics along railway sections or within a regional network, lacking the interaction analysis between local delay influences and conflict distribution at a microlevel. Meanwhile, delays are usually regarded as objectives in the rescheduling model, thus leading to a poor interpretability of output timetables where the dispatching strategies of each affected train are unclear. In general, the current research gap primarilylies in the coordination between local conflict resolution and global rescheduling for HSR train rescheduling. Faced with recoverable disturbances, this paper aims to present a feasible approach for global rescheduling considering conflict resolution costs and delay propagation influences, as well as an applicable framework from data input to result analysis.

The remainder of the paper is structured as follows: Section 2 presents the formulation of the rescheduling model. The conflict resolving and global optimizing algorithms are elaborated on in Section 3. To illustrate the effectiveness of proposed models and algorithms, Section 4 performs a case study followed by a dynamic delay analysis. Finally, Section 5 ends the paper with major contributions and possible future work.

2. Model Formulation

Under recoverable disturbances, given the basic data of primary delay characteristics, planned timetables, and resource allocation parameters, the current problem is how to realize the efficient rescheduling of the line section or the local network considering the closed-loop coordination among delay propagation, conflict detection, and strategy selection. The formulated model should consider the resolution strategy adaptability under different conflict states and the delay propagation influence under different dispatching strategies. In view of the complexity and difficulty of TTR, the proposed model is an integration of conflict resolution and global optimization, as shown in Figure 1.

2.1. Basic Assumptions. In order to both guarantee formulation rationality and solution efficiency, six basic assumptions have been made considering delay characteristics, dispatching experiences, operation regulations and etc.

Assumption 1: The abnormal scenario is a single-source disturbance. All trains operate punctually according to the planned schedule before the disturbance, and no other accident disturbance will occur during the rescheduling procedure under the current disturbance.

Assumption 2: The formulation targets one operation direction in a double-tracked HSR line. In case a bi-directional disturbance occurs, the problem can be solved by repeatedly loading the proposed models

when determining the primary train delay of each track direction.

Assumption 3: The station tracks in different directions are used independently. In the station yard, crossovers are equipped between different track directions for the convenience of train emergency operations. In order to avoid bi-directional delay influences and the mutual interference of arrival-departure operations, tracks in each direction are assumed to be used independently.

Assumption 4: The strategy of cancelling trains is excluded. Train cancellations are usually performed in scenarios of severe blockage or large-scale disturbance under infrastructure failure or bad weather. This paper focuses on the predictable disturbance scenario, where all trains can recover operation through timetable rescheduling. Meanwhile, in the daily dispatching management of HSR, cancelling trains is not recommended due to the fact that it may lead to traffic unbalance and circulation difficulty, which will greatly affect the quality of transportation services.

Assumption 5: The maximum affected time domain is no longer than 3 hours. On one hand, train dispatchers will release a phased rescheduling plan for the next 3 hours according to the HSR technical regulations. On the other hand, the number of maximum affected trains under recoverable delay disturbances is 21 in our dataset, with a duration time of 159 min.

Assumption 6: Accurate train speed control should be performed on all trains in the adjustment time domain. Basically, all conflict resolution strategies should follow a minimum time interval standard, which requires an explicit running time prediction of affected trains and unaffected trains. Once the departure or arrival time of a train is earlier or later than predicted, the theoretical conflict distribution will change, and the subsequent conflict resolution and delay propagation will be affected.

2.2. Conflict Resolving Mechanism

2.2.1. Resolution Strategies. The train conflicts on a double-track railway usually include the section conflict and the station conflict, where the arrival conflict, departure conflict, depart-arrive conflict, and arrive-pass conflict are involved in the station conflict. Due to the heterogeneity of conflict location, train grades, and resource allocation, the resolution strategies for various conflicts are different.

Taking the section conflict as an example, feasible strategies include organizing train avoidance, adjusting stop plan or dwelling time, organizing reverse operation, and adjusting section running speed, and the corresponding illustrations are indicated in Figure 2. The corresponding resolution equations and scenario constraints of different strategies can be established as follows:

(1) Organizing train avoidance. As illustrated in Figure 2(a), this strategy is recommended when the operation grade of succeeding train j is obviously
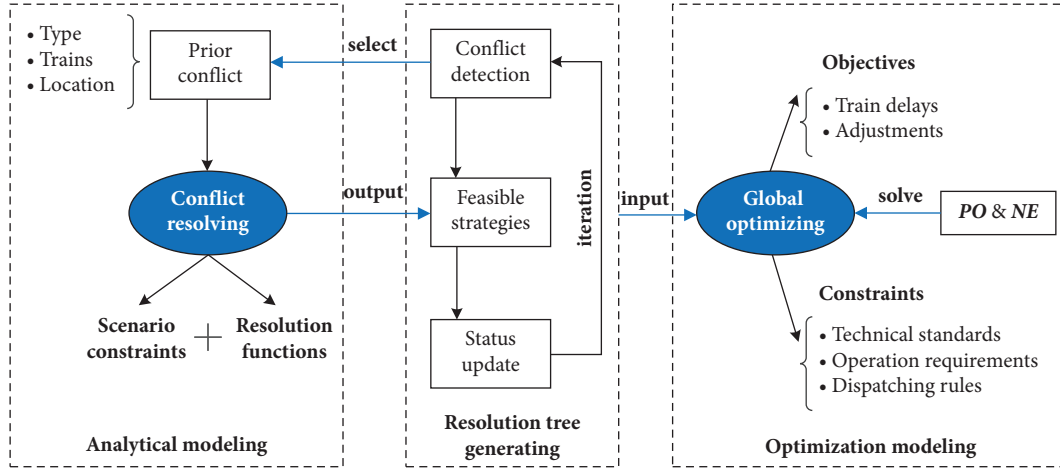
FIGURE 1: Integrated modeling of conflict solving and global optimizing.

higher than the preceding train i, and train i should avoid train j at the backward station k. The corresponding analytical expressions are shown in equation (1), where $x^A_{i,k}(t)$ and $x^D_{i,k}(t)$ denote the scheduled arrival time and departure time of train i at station k under the tth conflict resolution, while $t = 0$ refers to the planned time; $o^{k,k+1}_i$ is the running sequence order of train i in section $(k, k+1)$.

$$\begin{cases} x^A_{i,k}(t+1) = x^A_{i,k}(t), & x^A_{j,k}(t+1) = x^A_{j,k}(t), \\ x^D_{j,k}(t+1) = x^D_{j,k}(t), x^D_{i,k}(t+1) = x^D_{j,k}(t+1) + I^D_k, & \text{s.t. } o^{k,k+1}_i(t) = o^{k,k+1}_j(t) - 1, \\ o^{k,k+1}_i(t+1) = o^{k,k+1}_j(t), & o^{k,k+1}_j(t+1) = o^{k,k+1}_i(t). \end{cases} \tag{1}$$

(2) Adjusting the stop plan. This is a basic strategy to erase section conflict by postponing the departure time of succeeding train j regardless of its original stop plan at station k; see Figure 2(b). The corresponding resolution functions are established as follows:

$$\begin{cases} x^D_{j,k}(t+1) = x^D_{j,k}(t) + x^A_{i,k+1}(t) - x^A_{j,k+1}(t) + I^A_{k+1}, \\ x^A_{j,k+1}(t+1) = x^A_{j,k+1}(t) + x^D_{j,k}(t+1) - x^D_{j,k}(t). \end{cases} \tag{2}$$

(3) Organizing reverse operations. This strategy is recommended when the succeeding train is close to backward station k and the preceding train i has a longer section temporary stop; see Figure 2(c). Equation (3) shows the resolution functions and scenario constraints.

$$\begin{cases} x^D_{j,k}(t+1) = x^{k,k+1}_i(t) + w^{k,k+1}_i(t), \\ x^A_{j,k+1}(t+1) = x^A_{j,k+1}(t) + x^{k,k+1}_i(t) - x^D_{j,k}(t) + w^{k,k+1}_i(t), \end{cases} \tag{3}$$

$$\text{s.t.} 0 < x^{k,k+1}_i(t) - x^D_{j,k}(t) < \frac{2}{60}.$$

(4) Adjusting section running speed. This strategy can be applied when the arrival time difference at the forward station between two adjacent trains is relatively small; otherwise, it is suitable to apply other strategies to resolve the time difference, where the time difference is set at 1 min in the model, as indicated in equation (4). During the timetable rescheduling, the buffer times of section running should be sufficiently exploited; therefore, the speed adjustment should consider the preceding train despite slowing down the succeeding train, as indicated in Figure 2(d). However, the reduced time of the preceding train

$\Delta x^A_{i,k+1}$ is determined by its running buffer time and preceding headway redundancy; see equation (5). If the preceding train could not compress its section

running time by raising speed, the strategy is by nature slowing down the succeeding train when $\Delta x^A_{i,k+1}$ takes 0 according to equation (6).

$$\begin{cases} x^A_{i,k+1}(t) - x^A_{j,k+1}(t) \le \dfrac{1}{60}, \\[2mm] x^A_{i,k+1}(t+1) = x^A_{i,k+1}(t) - \Delta x^A_{i,k+1}, \\[2mm] x^A_{j,k+1}(t+1) = x^A_{j,k+1}(t) + \Delta x^A_{j,k+1}, \end{cases} \tag{4}$$

$$\Delta x^A_{i,k+1} = \min\left\{ \mathrm{buf}^{k,k+1}_i, x^A_{i,k+1}(t) - x^A_{l,k+1}(t) - I^A_{k+1} \right\}, o^{k,k+1}_l(t) = o^{k,k+1}_i(t) - 1, \tag{5}$$

$$\Delta x^A_{j,k+1} = x^A_{i,k+1}(t) - x^A_{j,k+1}(t) + I^A_{k+1} - \Delta x^A_{i,k+1}. \tag{6}$$

2.2.2. Tree-Based Strategy Path Generation. Under primary and secondary delay scenarios, the major conflict can be solved by different strategies, and different strategies will cause different subsequent delays and conflict distributions until the last affected train recovers operation or completes the operation service, thus forming different delay propagation chains.

(1) Strategy Tree Architecture. Based on the multitree method presented in the study [36], a tree-based conflict resolution mechanism is put forward, as indicated in Figure 3. Every tree node owns two kinds of status attributes: one is the cell recording parameters (denoted by P), such as the departure time, arrival time, stop scheme, operation sequence, conflict distribution, and section buffer time, and the other is the matrix recording the numbers of its sublayer resolution strategy branches (denoted by B). The index of an element in the parameter cell P is numbered in line with the node index in the resolution tree, and the number of strategies for a node is stored in the branch number matrix B.

Note that every element in array P is a matrix; e.g., in the cell of arrival time (denoted by P_{at}), element p_{ij} is the arrival time matrix of node c_{ij} before conflict resolution. By contrast, the element b_{ij} in matrix B is the number of selected strategies after the conflict resolution of node c_{ij}. Obviously, element 0 means there are no subsequent conflicts under the current strategy branch, and the sum of ith row elements equals the number of $i+1^{\text{th}}$ row elements. When b_{ij} is 0 for node c_{ij}, it means that the current node has achieved a conflict-free timetable, and it can be regarded as a convergent node. Meanwhile, it is indicated that different strategy paths converge at different nodes distributed at different levels, and the strategy tree will achieve global convergence when the sum of the ith row in B is 0.

(2) Resolution Tree Generation. The conflict between trains is by nature a contradiction of resource usage at the station or section. The conflict area is considered for the quantification of resolution costs. Due to the diversity of resolution

strategies, the strategies may perform in the station or the section adjacent to the location of the current conflict. To ensure the comparability and consistency of different strategies, the conflict area is composed of the current conflict position and adjacent stations. Specifically, the conflict area of a section (or station) includes the current section (or station) and adjacent stations. The resolution cost is defined as the weighted station delay within the conflict area. For the sake of minimizing the delay of trains with higher operation grades, when train i and train j conflict in a section $(k, k+1)$, the corresponding resolution cost rc is

$$rc = \sum_{l=k}^{k+1} \left(g_{il} \cdot \mathrm{delay}^l_i + g_{jl} \cdot \mathrm{delay}^l_j \right). \tag{7}$$

When train i and train j conflict at station k, the corresponding resolution cost is

$$rc = \begin{cases} \displaystyle\sum_{l=k}^{k+1} \left(g_{il} \cdot \mathrm{delay}^l_i + g_{jl} \cdot \mathrm{delay}^l_j \right), & k = 1, \\[3mm] \displaystyle\sum_{l=k-1}^{k+1} \left(g_{il} \cdot \mathrm{delay}^l_i + g_{jl} \cdot \mathrm{delay}^l_j \right), & k \in [2, m-1], \\[3mm] \displaystyle\sum_{l=k-1}^{k} \left(g_{il} \cdot \mathrm{delay}^l_i + g_{jl} \cdot \mathrm{delay}^l_j \right), & k = m. \end{cases} \tag{8}$$

Depending on the number of adaptable strategies, the following strategy selection rules for conflict resolution are designed:

(1) Select the unique strategy when there is only one adaptable strategy. The corresponding strategy branch should be retained, whatever the resolution cost.

(2) Select at least one strategy when there are two adaptable strategies. Let the two strategies be denoted by a_1 and a_2, and the resolution costs are rc_1
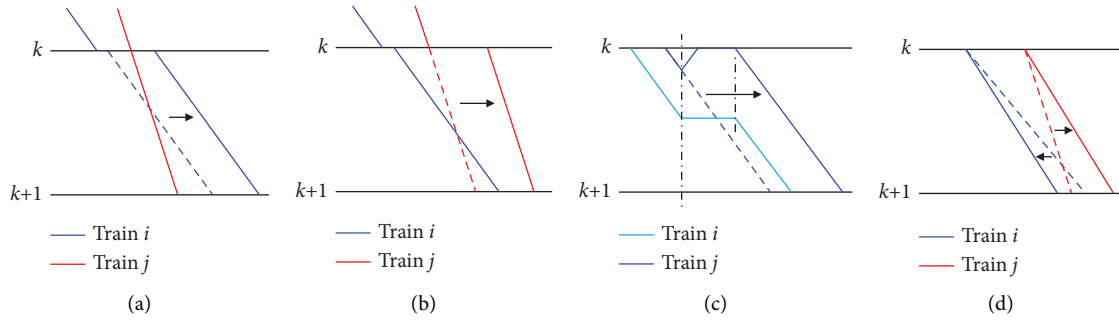
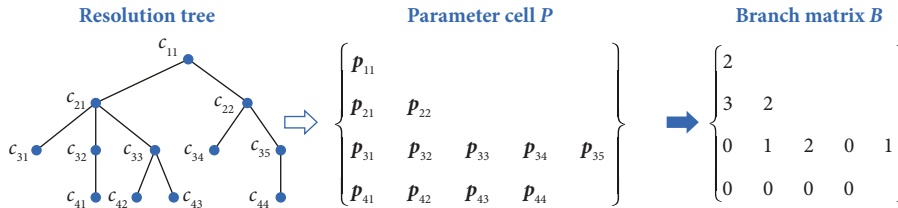FIGURE 2: Typical resolution strategies for the section conflict.

FIGURE 3: The architecture of the hierarchical database for a strategy tree.

and rc_2, respectively. Assuming that rc_1 is smaller than rc_2, if $rc_1 \leq 0.5rc_2$, strategy a_1 is superior to strategy a_2, and the current tree node generates a branch corresponding to a_1. Otherwise, there is no significant difference between a_1 and a_2, and both branches are retained in the strategy tree.

(3) Select at least two strategies when there are two adaptable strategies to guarantee the diversity of strategy paths. Let the three strategies be denoted by a_1, a_2, and a_3, and the resolution costs be rc_1, rc_2, and rc_3, respectively. The strategy selection should consider the trade-offs between the strategy with the highest cost and the strategy with the second highest cost. Assuming a_1 owns the high cost and a_3 owns the medium cost, if $rc_3 \leq 0.5rc_1$, strategy a_3 is superior to strategy a_1, and the current tree node should generate two branches corresponding to a_2 and a_3. Otherwise, strategy a_1 should be retained, namely generating three branches below the current tree node.

(3) Global Conflict Detection and Resolution (GCDR). The flowchart of GCDR is shown in Figure 4, which includes the following four key steps:

Step 1: Conflict resolution at the top node. The node in the top layer is unique under the influence of primary delay, and the corresponding conflict distributions are affected by the initial emergency measures. Obviously, the top node is not a convergent node, where the corresponding parameter cell is $P\{1, 1\}$. The number of strategy branches is $B(1, 1)$, and the parameter cell elements in row 2 are updated from $P\{2, 1\}$ to $P\{2, B(1, 1)\}$ accordingly.

Step 2: Global conflict-free judgement. A convergent node may occur at the second and lower layers, depending on the effects of resolution strategies. If the sum of b_{ij} in current row is 0, meaning that every terminal node has achieved a conflict-free status, then the GCDR algorithm ends; otherwise, the algorithm continues.

Step 3: Single conflict-free judgement. Before achieving global convergence, some resolution paths may realize a single conflict-free judgement in advance. For the xh^{th} node in layer ch, if its conflict distribution matrix $P_{sta}\{ch, xh\}$ is empty and the number of its strategy branches is 0, then it is a convergent node; otherwise, conflict selection and strategy resolution should be performed on the current node, and the corresponding parameters are updated.

Step 4: Element index calibration for the parameter cell. For a nonconvergent node (ch and xh), the calibration of its sublayer nodes should both consider the strategy branch distribution and the value of B (ch and xh).

2.3. Global Optimization Objectives. The direct manifestation of delay is the timetable deviation during train rescheduling, including the train departure deviation and arrival deviation. On one hand, the actual influences of trains with different operation grades are different when faced with the same delay. On the other hand, not all timetable deviations can be recognized as train delays because minor deviations are acceptable during daily operation. Therefore, the problem is formulated as a biobjective programming (BOP) model. The first objective (Obj_1) is formulated as a linear combination of delay judgement parameters and train delays:
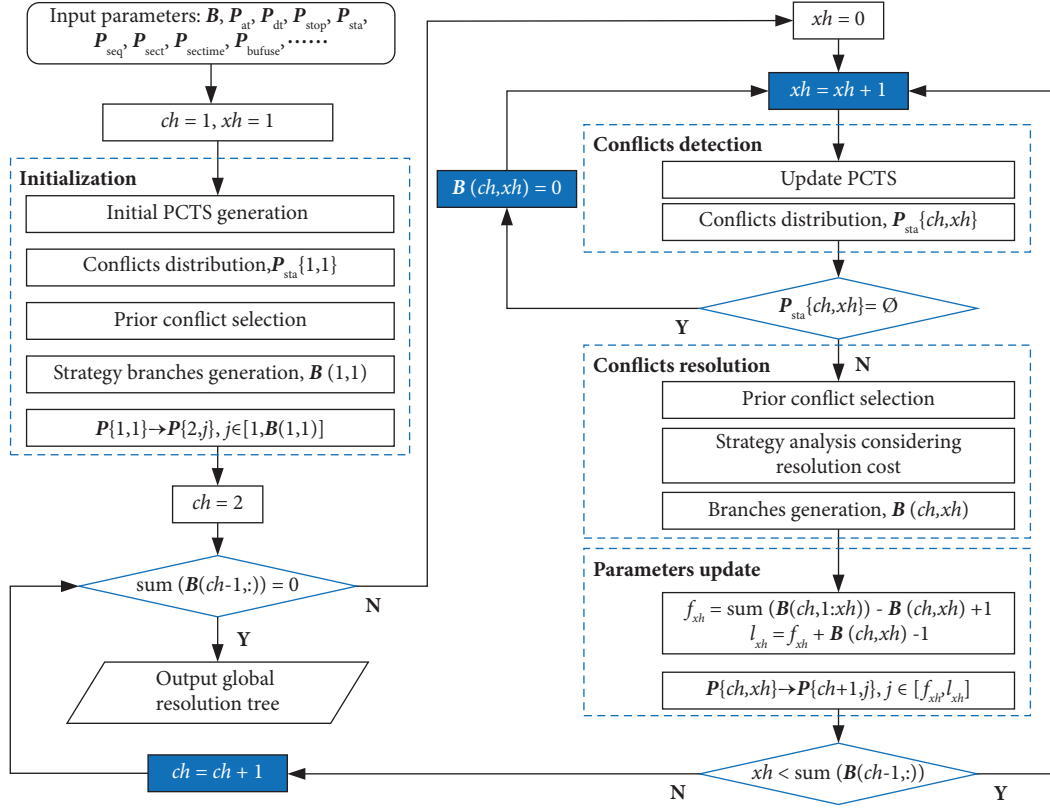
FIGURE 4: The framework of the GCDR algorithm.

$$\min \mathrm{Obj}_1 = \sum_{i=1}^{n} \sum_{k=1}^{m} g_{ik} \left[\alpha_{i,k}^A(t) \left(x_{i,k}^A(t) - x_{i,k}^A(0) \right) + \alpha_{i,k}^D(t) \left(x_{i,k}^D(t) - x_{i,k}^D(0) \right) \right], \tag{9}$$

where g_{ik} denotes the operation priority of ith train at the kth station, calculated by equation (10); n is the number of trains, and m is the number of stations; $\alpha_{i,k}^A(t)$ and $\alpha_{i,k}^D(t)$ are 0-1 binary variables denoting the delay status.

Train operation grades are key coefficients in both conflict resolution and global resolution. Generally, a train should be given a higher operation grade with a lower stopping frequency and a faster running speed. Meanwhile, to minimize the cumulative delay, long-haul trains deserve higher operation grades. Considering the factors of stopping frequency, running speed, and remaining operation range, the train operation grade is represented as follows:

$$g_{ik} = \frac{\eta_i \cdot \delta_{ik}}{\tau_i}, \tag{10}$$

where τ_i denotes the stopping frequency of train i; η_i denotes the designed speed grade; EMUs of the CR400 series, CRH2 series, and CRH300 series take 1.4, 1.2, and 1.0, respectively; δ_{ik} denotes the remaining range percentage of train i at station k. It can be seen that τ_i and η_i are static planned parameters, while δ_{ik} is a dynamic parameter varying with the train position and path.

Since this paper focuses more on the rescheduling procedure, the Obj_1 is established as an aggregated weighted delay at a macro level, while some research focuses on the arrival delay at terminal stations to enhance the punctuality rate.

According to Rule 204 of the *Railway Technical Management Rules* released by the China Railway Corporation, the timetable should pay attention to the integration of the train operation graph and passenger travel demand, as well as the coordination and equilibrium among different stations or sections. Targeting the scenario under recoverable disturbance without cancelling trains, the fewer the number of affected trains, the higher the average adjusting frequency will be, which will lead to a larger deviation from the planned timetable and a higher imbalance of resource utilization. Therefore, the second objective (Obj_2) aims at minimizing the average train adjusting frequency under the necessary constraint of the maximum number of affected trains.

$$\min \mathrm{Obj}_2 = \frac{1}{N_{\mathrm{aff}}(t)} \sum_{i \in \mathrm{Aff}(t)} \left(\sum_{k=1}^{m} res_i^k(t) + \sum_{k=1}^{m-1} res_i^{k,k+1}(t) \right), \tag{11}$$

where $\text{res}_i^k(t)$ and $\text{res}_i^{k,k+1}(t)$ are 0-1 variables, denoting the rescheduling status of train i at station k and section $(k, k+1)$, respectively; $A_{\text{ff}}(t)$ is the set of affected trains, and $N_{\text{aff}}(t)$ is the number of affected trains.

2.4. Model Constraints

2.4.1. Rescheduled Time Constraints. As mentioned in the conflict resolving section, there may exists several feasible resolution strategies for the same conflict, and some strategies will reschedule the departure time on the initialized timetable under disturbance. In most cases, the initialized departure time is usually later than the planned time, but it may shift earlier under the strategy of section headway compressing, station dwelling time reducing, and departure sequence reordering. In order to avoid unexpected deadlocks during resolving, necessary time constraints are inevitable.

(1) Departure time constraints. Since the train could not depart before the time printed on the tickets, the rescheduled departure time is not allowed to be earlier than the planned time.

$$x_{i,k}^D(t) \geq x_{i,k}^D(0), \forall i = 1, 2, \cdots, n; k \in [q_i, z_i]. \quad (12)$$

(2) Basic time interval constraints. The constraints should both consider the standards in the operation rules and the experiences during actual train dispatching. Because the standards are usually minimum values technically, the empirical values under historical disturbances are further considered, as indicated in Table 2. Based on the constraint value analysis, basic time interval constraints are listed in Table 3, where the last interval is to guarantee that there exists at least one available track for train j arriving at station k, with a minimum depart-arrive interval of 0.417 h (2.5 min).

2.4.2. Maximum Extra Avoidance Constraint. It is necessary to guarantee the priority of trains with high operation grades under the mixed running mode of trains with different operation speeds. However, it is inadvisable to successively avoid other superior trains for trains with lower operation grades in case the service quality worsens. Considering the running headway of HSR, the time loss of avoidance is about 10 min. The total avoiding time for a train should be controlled under 30 min; namely, the maximum avoidance frequency is 3. Considering there may be scheduled avoidance in the planned timetable, the extra avoidance frequency constraint is

$$\begin{cases} \text{Ng}_i(t) = o_i^{z_i-1,z_i}(t) + N_i^e(t) - o_i^{z_i-1,z_i}(0) - N_i^e(0) \leq 3, \\ N_i^e(t) = \text{card}\{j \mid x_{j,q_i}^D(0) > x_{i,q_i}^D(0), x_{j,k}^A(t) < x_{i,k}^A(t), x_{j,z_i}^A(t) = \text{NaN}\}, q_i \leq k < z_i, \\ N_i^e(0) = \text{card}\{j \mid x_{j,q_i}^D(0) > x_{i,q_i}^D(0), x_{j,k}^A(0) < x_{i,k}^A(0), x_{j,z_i}^A(0) = \text{NaN}\}, q_i \leq k < z_i, \end{cases} \quad (13)$$

where $\text{Ng}_i(t)$ denotes the extra avoidance frequency of train i under the tth conflict resolution; N_i^e denotes the number of trains overtaking train i and leaving the current dispatching section before the terminal station of train i, which will affect the operation sequence in the last section on the path of train i; q_i and z_i refer to the origin station and the terminal station of train i in the current dispatching section; $o_i^{k,k+1}$ is the running sequence order of train i in section $(k, k+1)$. Here, $k = z_i - 1$. NaN is the abbreviation for Not a Number. When the arrival time variable of a train is NaN, it means that the train has left the dispatching section before the current station.

Since the resolving model is the generation of the strategy tree, the maximum extra avoidance varies along different resolution paths. The constraint of maximum extra avoidance can greatly improve the global searching efficiency, which is the basis of branch pruning on the strategy tree in order to reduce the searching space for feasible resolution paths. Figure 5 shows an example of calculating avoidance frequency, where train 2 is taken as the analyzing object. Under the planned scheme, train 2 is only overtaken by train 3 at St_2; hence, the planned avoidance frequency is 1.

Under the rescheduled scheme, train 2 is successively overtaken by train 3 and train 4 at St_2, and by train 5 at St_4, hence the rescheduled avoidance frequency is 3. The extra avoidance frequency could not be directly calculated by the difference in running sequence in the last section because train 4 terminates its operation at St_4. Therefore, the extra avoidance under the rescheduled timetable should both consider the planned avoidance and the train path.

For the rescheduled timetable, the avoidance frequency of every train should satisfy the constraint, namely that we have

$$\max\{\text{Ng}_i(t) \mid i = 1, 2, \cdots, n\} \leq 3. \quad (14)$$

2.4.3. Delay Judging Threshold Constraint. During daily HSR operation, trains will not operate in accordance with the scheduled diagram. It is obvious that deviations below 3 min account for up to 93%; therefore, 3 min (0.05 h) is taken as the threshold value for distinguishing between acceptable deviation and train delay. The arrival delay and departure delay are judged by

TABLE 2: Constraint values of time intervals under actual dispatching scenarios.

Interval type	Arrival and departure	Arrive-pass and pass-depart	Section headway	Station dwelling
Actual operation graphs				
Empirical value	3~4 min	1~3 min	3~4 min	1~2 min
Constraint value	4 min	2 min	4 min	1 min

$$\alpha_{i,k}^A(t) = \begin{cases} 1, & \mathrm{Sgn}\left(x_{i,k}^A(t) - x_{i,k}^A(0) - 0.05\right) = 1, \\ 0, & \mathrm{Sgn}\left(x_{i,k}^A(t) - x_{i,k}^A(0) - 0.05\right) = -1 \text{ or NaN}, \end{cases} \tag{15}$$

$$\alpha_{i,k}^D(t) = \begin{cases} 1, & \mathrm{Sgn}\left(x_{i,k}^D(t) - x_{i,k}^D(0) - 0.05\right) = 1, \\ 0, & \mathrm{Sgn}\left(x_{i,k}^D(t) - x_{i,k}^D(0) - 0.05\right) = -1 \text{ or NaN}. \end{cases} \tag{16}$$

2.4.4. Maximum Number Constraint of Affected Trains. Based on equations (15) and (16), the number of affected trains under every rescheduled timetable can be calculated by equation (17), and the set of affected train descriptions is determined by equation (18).

$$N_{\mathrm{aff}}(t) = \sum_{i=1}^{n} \max\left\{\alpha_{i,k}^A(t), \alpha_{i,k}^D(t) \mid k \in [q_i, z_i]\right\}, \tag{17}$$

$$\mathrm{Aff}(t) = \left\{i \mid \max\left[\alpha_{i,k}^A(t), \alpha_{i,k}^D(t)\right] = 1, k \in [q_i, z_i]\right\}. \tag{18}$$

The maximum number of affected trains is constrained by the following constraint, where N_{aff}^* is the theoretical value of affected trains, estimated by the algorithm considering primary delay attributes and delay propagation characteristics presented in the literature [37], which is our former research.

$$N_{\mathrm{aff}}(t) \leq \lceil N_{\mathrm{aff}}^* \rceil. \tag{19}$$

2.4.5. Mapping Relationship Constraints. The mapping relationship constraint is used to identify the correlation between the train timetable and the conflict resolution path, where only a convergent conflict resolution path can generate a rescheduled timetable as the basis for global searching. This constraint is formulated as

$$\begin{cases} x_{i,k}^A(t) = P_{\mathrm{at}}\{ch, xh\}_{i,k}, \\ x_{i,k}^D(t) = P_{\mathrm{dt}}\{ch, xh\}_{i,k}, \forall i \in [1, n], k \in [q_i, z_i], \\ P_{\mathrm{sta}}\{ch, xh\} = \mathrm{NaN}, \end{cases} \tag{20}$$

where $P_{\mathrm{sta}}\{ch, xh\}$ is the conflict distribution status cell of a node (ch and xh), where ch and xh are the node's row number and sequence number in the resolution tree, respectively; when it takes NaN, the corresponding node is a terminal node of a conflict resolution path, and ch is a convergent layer; P_{at} and P_{dt} denote the scheduled arrival timetable array and the scheduled departure timetable array, respectively.

3. Algorithm Framework

3.1. Algorithm Applied for the Original Dispatching Section. The integrated algorithm framework dealing with train rescheduling in the original dispatching section is illustrated in Figure 6. There are five major processing steps:

Step 1: Algorithm inputting. The input data include disturbance characteristics, infrastructure resource allocation, and train operation data, where the disturbance characteristics are composed of occurring time, location, primary delay, first affected trains, and emergency measures. The infrastructure data contain station order, station mileage, track allocation, and

TABLE 3: Time interval constraints considered in the optimization model.

| #	Interval type	Constraint	Subject to
1	Departure interval	$x_{j,k}^D(t) - x_{i,k}^D(t) \geq 0.067$ $k \in [1, m-1]$	$\begin{cases} o_j^{k,k+1}(t) = o_i^{k,k+1}(t) + 1 \\ i,j \in \{i \mid x_{i,k}^A(t) < x_{i,k}^D(t)\} \end{cases}$
2	Arrival interval	$x_{j,k}^A(t) - x_{i,k}^A(t) \geq 0.067$ $k \in [2, m]$	$\begin{cases} o_j^{k-1,k}(t) = o_i^{k-1,k}(t) + 1 \\ i,j \in \{i \mid x_{i,k}^A(t) < x_{i,k}^D(t)\} \end{cases}$
3	Arrive-pass interval	$x_{i,k}^A(t) - x_{j,k}^A(t) \geq 0.033$ $k \in [2, m]$	$\begin{cases} x_{i,k}^A(t) < x_{j,k}^P(t) < x_{i,k}^D(t) \\ x_{j,k}^D(t) = x_{j,k}^A(t) = x_{j,k}^P(t) \end{cases}$
4	Pass-depart interval	$x_{i,k}^D(t) - x_{j,k}^D(t) \geq 0.033$ $k \in [1, m-1]$	$\begin{cases} x_{i,k}^A(t) < x_{j,k}^P(t) < x_{i,k}^D(t) \\ x_{j,k}^D(t) = x_{j,k}^A(t) = x_{j,k}^P(t) \end{cases}$
5	Station dwelling interval	$x_{i,k}^D(t) - x_{i,k}^A(t) \geq 0.0167$ $k \in [1, m]$	$i \in \{i \mid x_{i,k}^A(t) < x_{i,k}^D(t)\}$
6	Depart-arrive interval	$\mathrm{card}\left\{ i \,\middle|\, \begin{array}{c} x_{i,k}^A(t) < x_{j,k}^A(t), x_{i,k}^A(t) < x_{i,k}^D(t), \\ x_{i,k}^D(t) + 0.417 > x_{j,k}^A(t) \end{array} \right\} \leq r_k - 1$ $k \in [1, m-1]$	r_k is the number of arrival-departure tracks in the current direction at station k
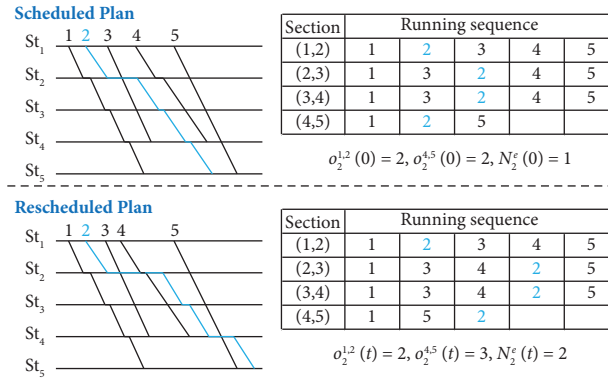
FIGURE 5: A simple illustration of avoidance frequency calculation.

network topology. The train operation data consist of a planned timetable, running path, operation level, and buffer time.

Step 2: Strategy resolving. This step is by nature a microcirculation of conflict detection and strategy resolution, where the former is used to recognize key conflicts, considering dominance and priority, and the latter is applied to analyze feasible resolution strategies and update relevant parameters. Meanwhile, the resolution tree is simultaneously generated considering the strategy branch selection rules.

Step 3: Global optimizing. On the basis of strategy resolving, the current step is responsible for deciding a convergent resolution path with global optimality and equilibrium, consisting of the DFS-based pruning, the Pareto front generating, and the Nash equilibrium finding.

Step 4: Parameter extracting. Parameters such as train arrival time, departure time, running headway, and operation sequence should be extracted immediately as the basis of dynamic conflict resolution, the support of scenario parameter calibration, and the assistance of strategy evaluation.

Step 5: Algorithm outputting. The output data include the optimal resolution strategy path, the rescheduled train timetables coordinated with the resolution strategy path, and the values of two objectives under the optimal solution. Other data, such as station delay, number of affected trains, and train avoidance frequency, can be extracted from the extra statistics.

3.2. Algorithm Applied for the Adjacent-Affected Dispatching Section. Considering the complexity of rail-net topology and the diversity of train running paths, train delays may propagate across adjacent dispatching sections and form part of network propagation. The following two jobs should be performed when dealing with this kind of trans-section propagation:

(1) Determine the adjacent-affected dispatching sections. The original affected dispatching section may have two or more adjacent dispatching sections,

while it should be noted that not every adjacent section would suffer from the primary delay or secondary delay occurring in the original dispatching section, and the train delay would propagate across several dispatching sections when the disturbance is severe or happens near a junction station. Taking the delayed trains in the current dispatching section as analyzing objects, the adjacent affected dispatching sections are determined according to the running path and entering delay of affected trains.

(2) Initialize the timetables of affected dispatching sections. Under the influence of delayed trans-section trains, the departure sequence at the origin station in an affected dispatching section will be disarrayed accordingly, and the corresponding departure time interval or depart-arrive time interval may not meet the minimum technical standards. Therefore, during the timetable initialization of an affected dispatching section, the departure sequence and time at its origin station are first rescheduled under minimum time interval standards, and then the subsequent operation lines are updated recursively based on the planned section running time and station dwelling time.

The initialized timetable is seldom a conflict-free timetable, especially in the dispatching section with a higher service frequency. As indicated in Figure 7, the blue solid lines in the "delayed trans-in trains" represent the shifted operation diagram of train 2 and train 4, which are affected trains in the upstream dispatching section, where trans-in trains refer to the trains transferring from adjacent connected railway sections into the current dispatching section. The purpose of initializing the timetable is only to erase the departure conflicts at the first station, St_1, regardless of the conflicts at forward stations, and then the initialized timetable can be used as the basis for subsequent conflict resolution. The above-mentioned algorithm for a single dispatching section should be loaded repeatedly to perform conflict detection, strategy resolution, and global optimization, where a mapping relationship should be established because the initialized departure sequence is different from the planned departure sequence.
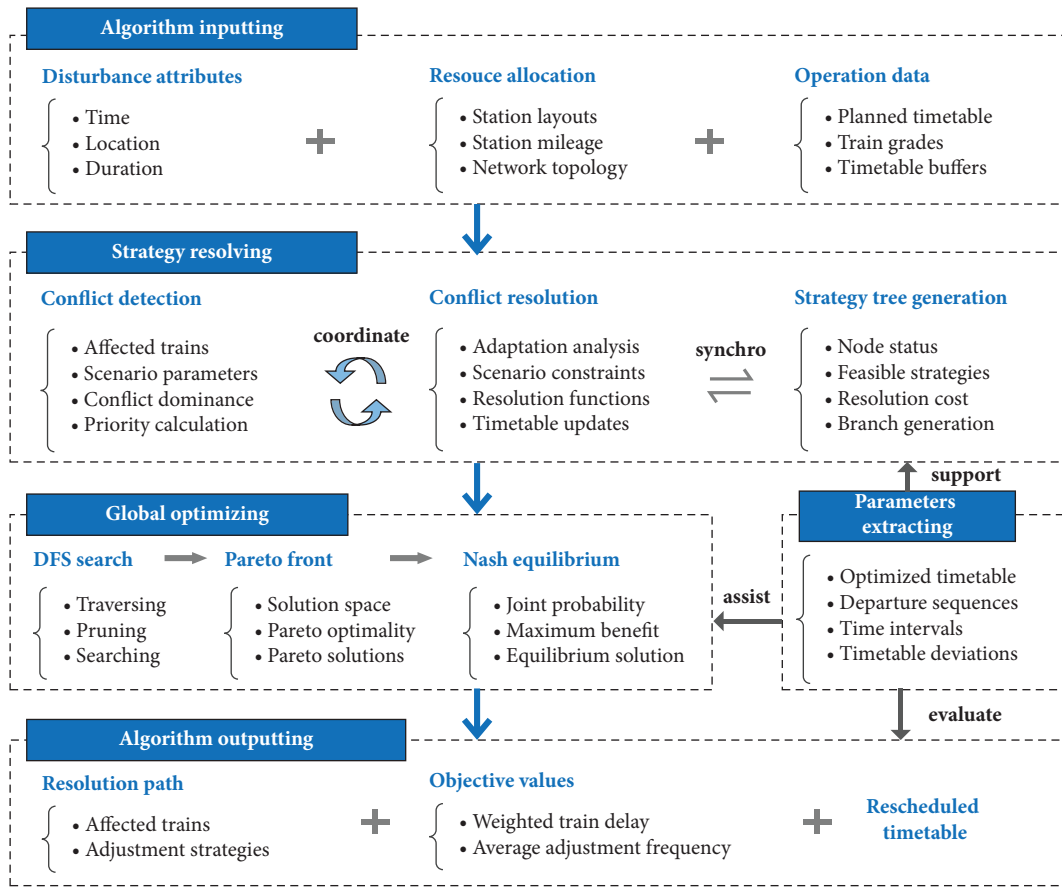
FIGURE 6: The integrated rescheduling algorithm framework for the original section.

(a)   (b)   (c)
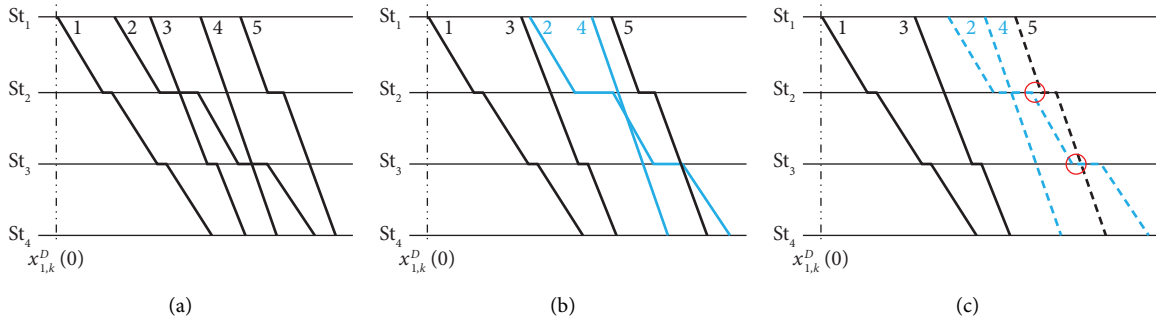
FIGURE 7: Possible conflicts distribution after timetable initialization. (a) Planned train timetable. (b) Delayed trans-in trains. (c) Initialized train timetable.

3.3. Input Data Processing

3.3.1. Data Composition.
The data used in this study were provided by the Shanghai Railway Bureau. Generally, the data can be split into the infrastructure data and the operation data, as shown in Figure 8. The infrastructure data are composed of the regional railway network topology, the station layout, the speed limit distribution, and the line alignment. The operation data cover the disturbance event scenario, the train parameters, the original and rescheduled plans, and the station delay statistics.

3.3.2. Data Preprocessing.
The preprocessing of original data mainly includes the following tasks:

(1) Disturbance attribute extraction. Extract the disturbance attributes from the basic dataset, including the time and location of occurrence, the disturbance causes, the first affected train, and the disturbance duration.

(2) Operation parameter extraction. Based on the planned timetable, extract the buffer time distribution of both the section running and the station
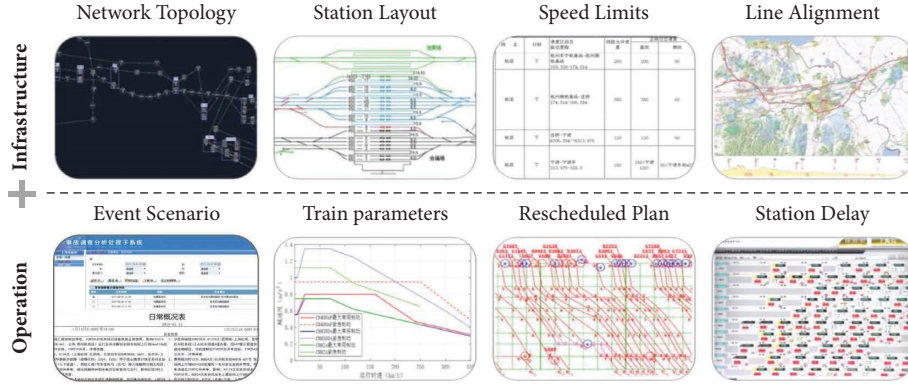
FIGURE 8: Basic input data composition.

dwelling for each train, the stop scheme and the running path of each train, and the departure sequence at each station.

(3) Physic parameter extraction. Establish the arrays of speed upper bounds, arrival-departure tracks, and train acceleration and deceleration rates.

3.4. Solution Algorithm

3.4.1. DFS-Based Pruning Algorithm. When finding the optimal path in the strategy tree generated during conflict resolution, it is necessary to choose an appropriate path-searching algorithm to traverse the graph. Meanwhile, strategy branches with inferior performance or poor feasibility need to be pruned together with their sublayer nodes and links. Traditionally, there are two searching methods: depth-first searching (DFS) and breadth-first searching (BFS), as shown in Figure 9. The DFS is competent for searching for all feasible solutions, and the BFS is usually used for searching for optimal solutions. Since the proposed optimizing model is biobjective programming and the BFS could not find a resolution path with both objectives of optimality, a combination of DFS searching and strategy brunch pruning is more appropriate in this study.

During the DFS searching in a conflict resolution tree, once the rescheduled timetable under a node does not meet the constraints of maximum train avoidance and maximum affected train number, the current node and subsequent branches are pruned from the resolution tree in order to narrow the solution space for global searching. Taking the maximum train avoidance as an example, its pseudocode is shown in Algorithm 1.

3.4.2. Embedded Probability Model Based on Nash Equilibrium. The global solution is formulated as a BOP model, where the objectives of weighted train delay and average train adjustment frequency cannot achieve their optimal simultaneously under realistic disturbance scenarios, thus leading to the nonuniqueness of optimal solutions. In view of this, the method of Pareto Optimality has been introduced into the solving process [38]. The current problem can be seen as noncooperative gaming (NCG) between two objectives. Accordingly, the theory of Nash equilibrium is applied here to find an optimal solution from the Pareto front, which outperforms other solving methods such as linear weighting or stratified sequencing in subjectivity and compatibility for the current BOP model. The search for the equilibrium point can be transformed into the optimization problem of joint probability distribution within the Pareto front. The Nash equilibrium solving model is formulated as

$$\max \text{Nash}\left(\mathbf{S}_1, \mathbf{S}_2, \cdots, \mathbf{S}_{N_{\text{obj}}}: u_1, u_2, \cdots, u_{N_{\text{obj}}}\right) = \sum_{i=1}^{N_{\text{obj}}}\left[u_i - \sum_{j=1}^{N_{\text{pf}}}\left(f_{ij} \cdot \prod_{i=1}^{N_{\text{obj}}} s_{ij}\right)\right], \tag{21}$$

$$\text{s.t.} \begin{cases} \sum_{j=1}^{N_{\text{pf}}} s_{ij} = 1 & i = 1, 2, \cdots, N_{\text{obj}}, \\ u_i - \sum_{j=1}^{N_{\text{pf}}} f_{ij}s_{ij} \geq 0 & i = 1, 2, \cdots, N_{\text{obj}}, \\ s_{ij} \geq 0 & i = 1, 2, \cdots, N_{\text{obj}}; j = i = 1, 2, \cdots, N_{\text{pf}}, \end{cases} \tag{22}$$
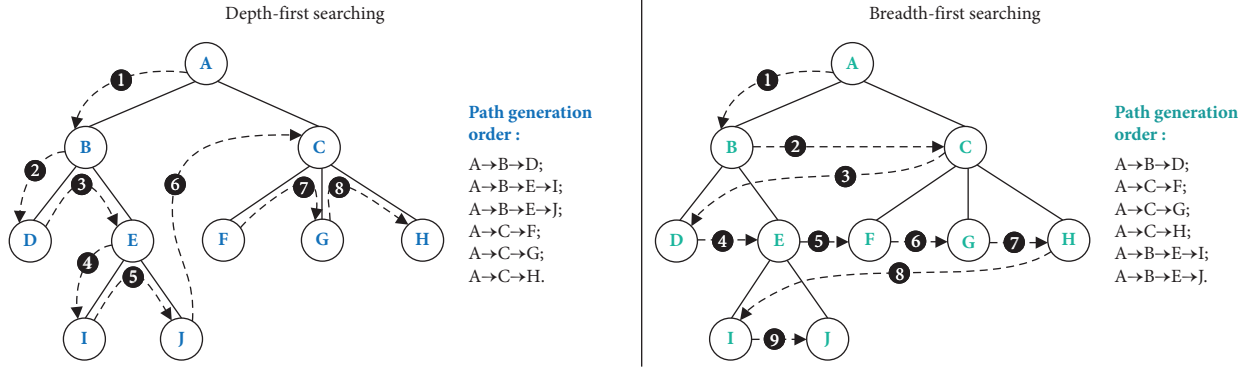
FIGURE 9: The mechanism of DFS and BFS methods.

Input: One rescheduled timetable under a resolution path, T_{re}; The original planned timetable, T_p; Number of potential affected trains, n; Number of stations along the dispatching section, m.
(1) Extract the departure and arrival time matrix from T_{re} and T_p, output $X_a(t)$, $X_d(t)$, $X_a(0)$, and $X_d(0)$
(2) Extract the stop scheme matrix ST, the rescheduled section running sequence matrix $\mathbf{RS}$, and the original section running sequence matrix OS
(3) **for** $i = 1$ to n **do**
(4) $\quad ST(i) = ST(:, i)$
(5) $\quad$ Extract the train path origination q_i and destination z_i according to $ST(i)$
(6) $\quad$ Modify q_i and z_i considering trans-section trains and short routing trains
(7) $\quad RSv = \mathrm{rm\ missing}(RS(z_i - 1, :))$ % remove null elements
(8) $\quad o_i^{z_i-1,z_i}(t) = \mathrm{find}(RSv == i)$ % identify the rescheduled terminal arriving sequence of train i
(9) $\quad OSv = \mathrm{rm\ missing}(OS(z_i - 1, :))$ % remove null elements
(10) $\quad o_i^{z_i-1,z_i}(0) = \mathrm{find}(RSv == i)$ % identify the planned terminal arriving sequence of train i
(11) $\quad$ **for** $j = 1$ to n **do** % consider trains overtaking train i and leaved current section before z_i
(12) $\quad\quad$ Update the rescheduled set of trains with trajectory lines crossing train i, CR_r
(13) $\quad\quad$ Update the planned set of trains with spatiotemporal trajectory lines crossing train i, CR_p
(14) $\quad$ **end for**
(15) $\quad$ Initialize $N_i^e(t) = 0$, $N_i^e(0) = 0$
(16) $\quad$ **for** $k = 1$ to $\mathrm{size}(CR_r, 2)$ **do**
(17) $\quad\quad$ **if** is $\mathrm{nan}(X_a(t)(z_i, CR_r(k))) == 1$ **do**
(18) $\quad\quad N_i^e(t) = N_i^e(t) + 1$
(19) $\quad\quad$ **else do** $N_i^e(t) = N_i^e(t)$
(20) $\quad\quad$ **end if**
(21) $\quad$ **end for**
(22) $\quad$ Update $N_i^e(0)$ according to $X_a(0)$ and CR_p, similar to steps 16 to 21
(23) $\quad \mathrm{Ng}_i(t) = o_i^{z_i-1,z_i}(t) - o_i^{z_i-1,z_i}(0) + N_i^e(t) - N_i^e(0)$
(24) **end for**
(25) $\mathrm{Ng}_m(t) = \max\{\mathrm{Ng}_i(t) \mid i = 1, 2, \cdots, n\}$ %calculate the maximum extra train avoidance frequency

ALGORITHM 1: Calculation of maximum extra train avoidance frequency.

where N_{obj} is the number of objectives, N_{pf} is the number of Pareto solutions, S_i is the 1-by-N_{pf} row vector of probability distribution under the ith objective, f_{ij} denotes the normalized value of the jth solution for the ith objective to erase the dimension difference, and u_i is the expected upper bound of normalized values for the ith objective. Note that S_i is the distribution vector of different Pareto solutions under the ith objective, where the element s_{ij} corresponds to the choice probability of Pareto solution x_j to objective Obj_i.

The pseudo-code for integrated Pareto front generation and Nash equilibrium solution is listed in Algorithm 2.

4. Case Analysis and Discussion

4.1. Scenario Description. According to the database of event records provided by the Shanghai Railway Bureau, a typical disturbance occurring in the section between the station *Suzhoudong* and the station *Bengbunan* on the Beijing–Shanghai HSR is taken as the real-case scenario. The disturbance happens at 10:05 a.m. and leads to a temporary section blockage of 35 min. The first affected train is G1965, and the initial emergency measures are a section temporary stop and speed limitations. Under this disturbance, the forward running paths of potential affected trains can better

Input: The set of s terminal tree nodes on all convergent resolution paths, $\mathbf{S}_{\text{tr}}$;
The set of rescheduled timetables under all terminal tree nodes, $\mathbf{T}_{\text{re}}$;
The original planned timetable, T_p; Acceptable number of affected trains N_{aff}^*
(1) **for** $k = 1$ to s **do**
(2) $ch = \mathbf{S}_{\text{tr}}(k, 1)$, $xh = \mathbf{S}_{\text{tr}}(k, 2)$
(3)   Calculate maximum extra train avoidance of affected train $Ng_m(k)$, according to $T_{\text{re}}(k)$ and T_p
(4)   Calculate the maximum number of affected trains $N_{aff}(k)$, according to $T_{\text{re}}(k)$ and T_p
(5)   **If** $Ng_m(k) > 3$ or $N_{aff}(k) > N_{\text{aff}}^*$ **do**
(6)   continue
(7)   **else do**
(8)   Calculate Obj_1 and Obj_2 according to equations (9) and (11)
(9)   Update the *solution* space with $[ch, xh, \text{Obj}_1, \text{Obj}_2]$
(10)   **end if**
(11) **end for**
(12) Calculate the number of updated solutions, n_{fes}; Extract the objective values, Obj
(13) $pfx = \text{ones}(n_{\text{fes}}, 1)$% define a judgement vector, with each element taking the initial value of 1
(14) **for** $i = 1$ to n_{fes} **do**
(15)   **for** $j = 1$ to n_{fes} **do**
(16)   **if** $Obj(i, 1) > Obj(j, 1)$ and $Obj(i, 2) > Obj(j, 2)$ **do**
(17) $pfx(i) = 0$
(18)   **end if**
(19)   **end for**
(20) **end for**
(21) $pf = \text{find}(pfx == 1)$ %find the location of solutions with pareto optimality
(22) $pf_{\text{sta}} = solution(\text{pf}, :)$ %extract the attributes of pareto solutions
(23) $\text{Obj}_{\text{pf}} = pf_{\text{sta}}(\text{pf}, [3, 4])$; $n_{\text{obj}} = 2$; $n_{\text{pf}} = \text{size}(Obj_{\text{pf}}, 1)$
(24) $f_{\text{obj}} = Obj_{\text{pf}}^T$, $f_{\text{obj}} = \text{mapminmax}(f_{\text{obj}}, 0.1, 1)$ %Normalize the objective value
(25) Generate the initial probability distribution matrix S, $S_0 = \text{rand}(2 \times n_{\text{pf}}, 1)$
(26) Decide the upper expectation bound of two objectives, u_1 and u_2
(27) Define the linear equality constraints and inequality constraints in equation (22) $\mathbf{A1} = \text{ones}(1, n_{\text{pf}})$; $\mathbf{A0} = \text{zeros}(1, n_{\text{pf}})$; $\mathbf{Aeq} = [\text{A1},$
     $\text{A0}; \text{A0}, \text{A1}]$; $\mathbf{beq} = \text{ones}(n_{\text{obj}}, 1)$. $\mathbf{A} = [f_{\text{obj}}(1, :), \text{A0}; \text{A0}, f_{\text{obj}}(2, :)]$; $\mathbf{b} = [u_1; u_2]$; $\mathbf{slb} = \text{zeros}(1, n_{\text{obj}} \times n_{\text{pf}})$; $\mathbf{sub} = []$
(28) Write the objective function based on pareto solutions according to equation (21)
(29) $[S, \text{objv}, \text{exitflag}] = \text{fmincon}(\text{fun}, S_0, \mathbf{A}, \mathbf{b}, \mathbf{Aeq}, \mathbf{beq}, \mathbf{slb}, \mathbf{sub})$ %exitflag = 1
(30) $S_{\text{re}} = [S(1 : n_{\text{pf}}), S(n_{\text{pf}} + 1 : 2n_{\text{pf}})]$ % recombine the output results
(31) $S_{\text{ave}} = \text{mean}(S_{\text{re}}, 2)$, $L_{\text{nash}} = \text{find}(S_{\text{ave}} == \text{max}(S_{\text{ave}}))$ %find the location of equilibrium solution

ALGORITHM 2: Pareto front generation and Nash equilibrium solution.

cover different adjacent dispatching sections. The network topology of relevant dispatching sections is shown in Figure 10, where the *Hefei–Bengbu* PDL (passenger dedicated line) also functions as a connection line between *Beijing–Shanghai* HSR and other HSRs, despite the fact that it is under an independent dispatching mode. The basic parameters under current disturbance are listed in Table 4, and the initialized timetable of the original dispatching section under current disturbance is shown in Figure 11.

4.2. Algorithm Outputs

4.2.1. Original Dispatching Section. The value distribution of two objectives is shown in Figure 12. With the increase in the strategy layer, the mean value of weighted train delay maintains 315~320 h, while the gap between the maximum value and the minimum value is getting wider. Similarly, the minimum value of the average adjusting frequency fluctuates between 5.2 and 5.35 times, while the mean value and the maximum value are gradually increasing.

Based on the subsequent strategy of branch pruning, the algorithm outputs 998 feasible solutions. After global Pareto front searching, 228 Pareto solutions were finally obtained. Figure 13 shows the rescheduled train diagram of the original affected dispatching section from *Xuzhoudong* to *Nanjingnan*.

4.2.2. Adjacent-Affected Dispatching Section. According to the computational results, five forward dispatching sections are affected more or less by the disturbance events. Taking *Nanjing–Hangzhou* HSR as an example, the initialized timetable under delayed trains-in trains from *Xuzhoudong* to *Nanjingnan* section is indicated in Figure 14, where another 8 trains are delayed in varying degrees successively under the influence of nine delayed trans-in trains. After global conflict resolution and optimization, there are 17,851 convergent strategy paths in the resolution tree. Through strategy pruning and Pareto front searching, 106 Pareto solutions are generated, as shown in Figure 15. The 101st Pareto solution (the 15, 156th feasible
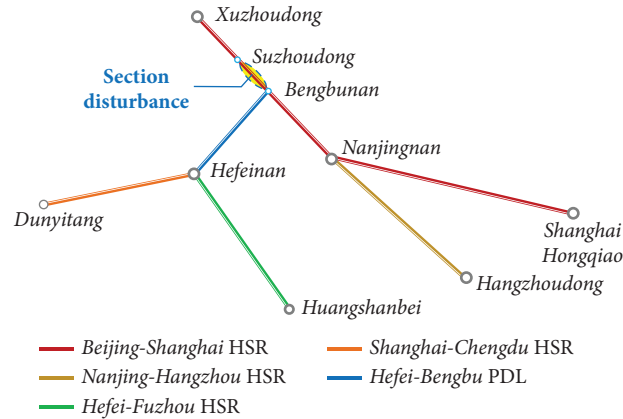
FIGURE 10: The topology of potential affected dispatching sections.

TABLE 4: Disturbance scenario parameters of the original dispatching section.

Parameter	Symbol	Value	Notes
Station number	$[1, m]$	(1, 6)	From Xuzhoudong to Nanjingnan
Occurring location	$(k, k+1)$	(2, 3)	Between Suzhoudong and Bengbunan
Location mileage	l_0	111.2 km	Away from the Xuzhoudong station
Occurring time	t_0	10.083 h	—
Primary delay	$delay_{1,3}^A$	0.583 h	The arrival delay of G1965 at the Bengbunan station
Maximum affected trains	N_{aff}^*	22	Determined by the historical data, including the first affected train
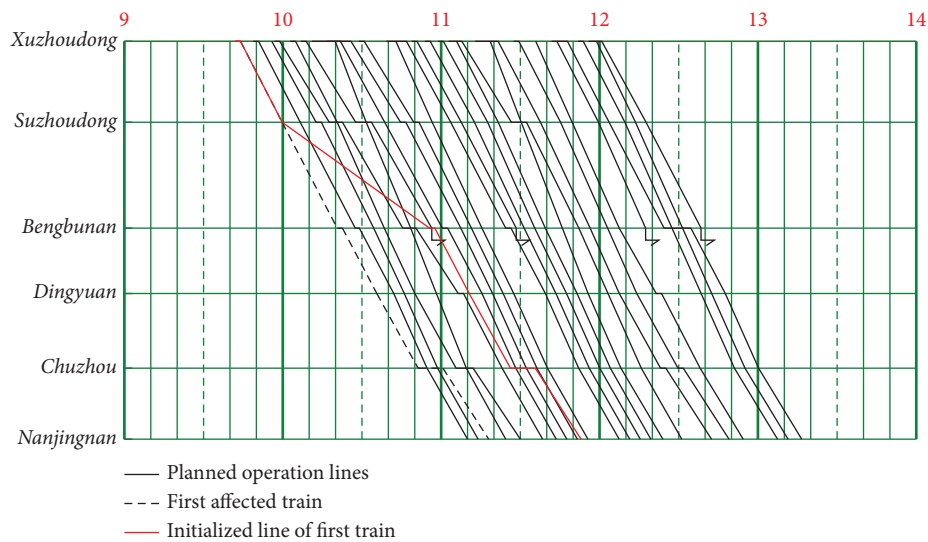
FIGURE 11: Initialized timetable of the original dispatching section under current disturbance.

solution) is verified to be the Nash equilibrium solution, with a global weighted train delay of 581.99 h and an average train adjustment frequency of 8.69 times. The rescheduled timetable is illustrated in Figure 16, and the corresponding running sequence adjustments are depicted in Table 5, which is considered to be a reasonable scheme under the maximum train avoidance constraint (see equation (14)).
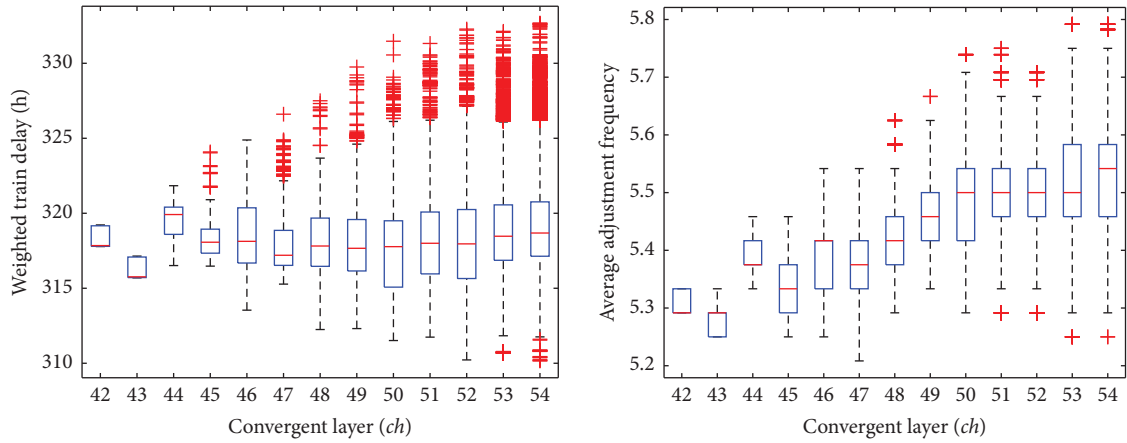
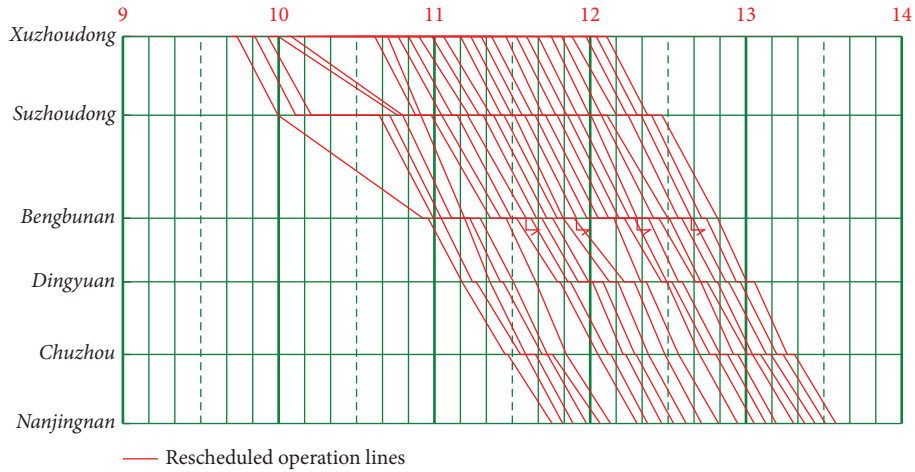FIGURE 12: The box plot of two objective distributions of convergent layers (*Xuzhou–Nanjing*).

— Rescheduled operation lines

FIGURE 13: The rescheduled train operation diagram of the original section under disturbance.
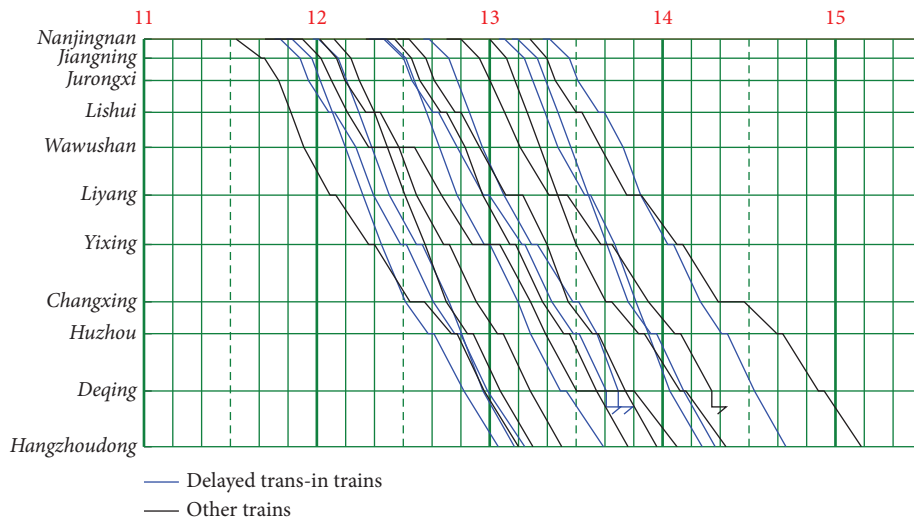

— Delayed trans-in trains
— Other trains

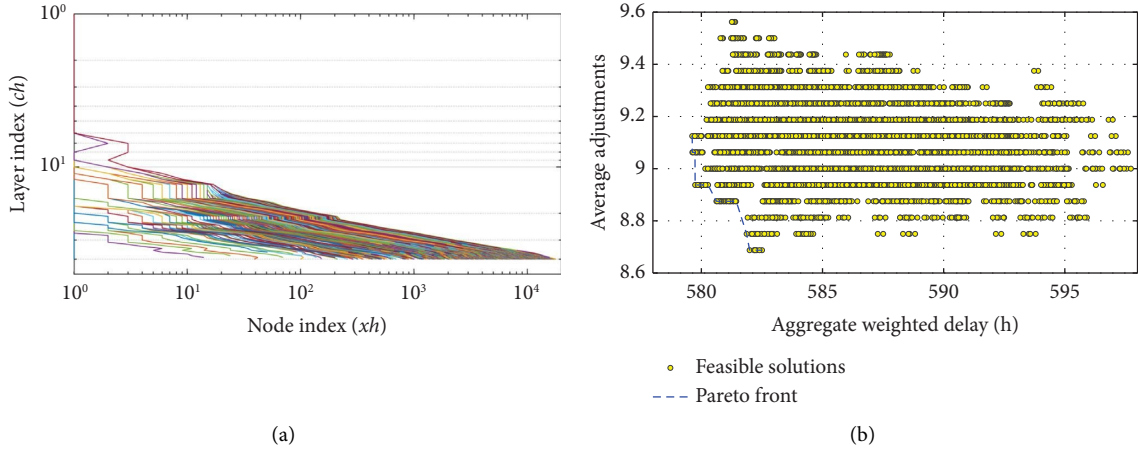FIGURE 14: Conflicted timetable of *Nanjing–Hangzhou* HSR under delayed trans-in trains.

(a)

(b)

FIGURE 15: The distribution of (a) resolution paths and (b) Pareto solution (*Nanjing–Hangzhou*).

Rescheduled trans-in trains
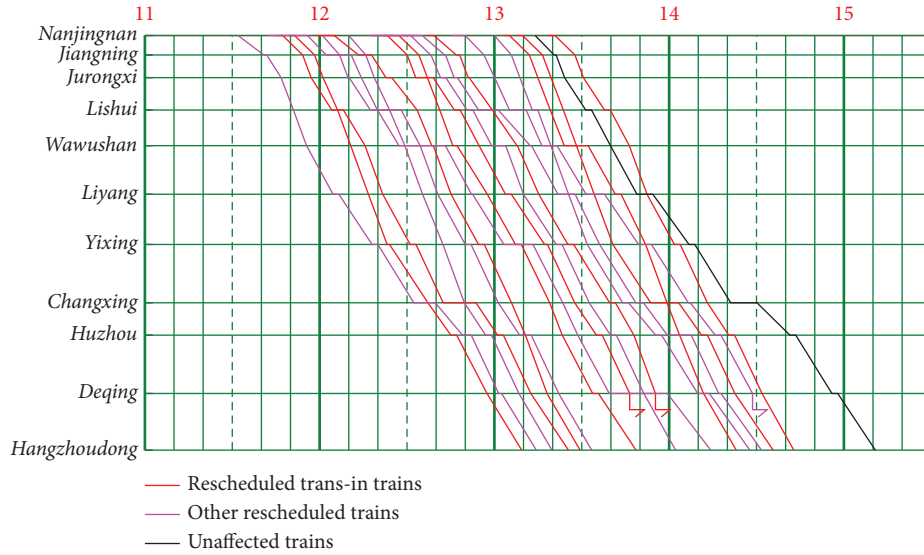Other rescheduled trains
Unaffected trains

FIGURE 16: The rescheduled train operation lines of *Nanjing–Hangzhou* HSR.

TABLE 5: The rescheduled station departure sequences of *Nanjing–Hangzhou* HSR.

Section	Train departure sequence																
(1, 2)	1	2	3	4	6	5	7	8	9	10	11	12	13	14	15	16	17
(2, 3)	1	2	3	6	4	7	5	8	9	10	11	12	13	14	15	16	17
(3, 4)	1	2	3	6	4	7	5	9	8	10	11	12	13	14	15	16	17
(4, 5)	1	3	2	4	7	6	5	9	8	10	12	11	13	14	15	16	17
(5, 6)	1	3	2	7	6	5	4	9	8	10	12	11	14	13	16	15	17
(6, 7)	1	3	2	7	6	5	4	9	8	10	12	14	11	16	13	15	18
(7, 8)	1	3	2	7	6	5	9	4	8	10	12	14	11	16	15	13	18
(8, 9)	3	1	7	2	6	5	9	4	8	10	12	14	11	15	16	13	18
(9, 10)	3	1	7	2	5	6	9	4	8	10	12	14	15	11	16	13	18
(10, 11)	3	1	7	2	5	6	9	8	10	12	4	15	14	11	16	13	18

4.3. Network Delay Propagation

4.3.1. Train Delay Indicators.
In order to deeply analyze the delay propagation characteristics during conflict resolution, the cumulative delay (*CD*) and instantaneous delay (*ID*) have been put forward as two evaluation indicators.

(1) Cumulative Delay. During the time period from the disturbance start time x_{acc}^{start} to a certain time x_T, the cumulative delay of an affected train i is defined as the sum of its station departure delay, as indicated in equation (23) It should be noted that the arrival time may be earlier than the planned time due to the implementation of retiming or

reordering, while the deviation of departure time is always a non-negative value according to the operation rules, and that is why the departure time is adopted to calculate *CD*.

$$\mathrm{CD}_{i,T} = \sum_k \left(x_{i,k}^D(t) - x_{i,k}^D(0) \right), k \in \left\{ k \mid x_{\mathrm{acc}}^{\mathrm{start}} < x_{i,k}^D(t) \leq x_T \right\}. \tag{23}$$

(2) Instantaneous Delay. The instantaneous delay of an affected train i is defined as the non-negative deviation between the rescheduled operation line and the planned operation line at a certain time x_T. The deviation is calculated according to the relative spatiotemporal position. As indicated in Figures 17(a) and 17(b), if the timeline intersects

the rescheduled operation line at a station k, *ID* is composed of departure delay and dwelling deviation, which can be transformed into the deviation between x_T and planned departure time, as indicated in equation (24) According to Figures 17(c)–17(f), if the point of intersection lies in the section $(k, k+1)$, *ID* depends on the intersected location and the rescheduled strategy. $x_{i,l}(0)$ denotes the planned passing time at location l, and it is calculated by equation (25) when the rescheduled operation line appears without a section temporary stop and by equation (26) depending on the position relationship between x_T and $x_i^{k,k+1}(t)$ under a temporary stop. Besides, when x_T is earlier than the planned time or the rescheduled train i has terminated before x_T, the *ID* turns to 0.

$$\mathrm{ID}_{i,T}^k = \begin{cases} x_T - x_{i,k}^D(0), & x_T > x_{i,k}^D(0), \\ \\ 0, & x_T \leq x_{i,k}^D(0), \end{cases} \tag{24}$$

$$x_{i,l}(0) = x_{i,k}^D(0) + \left(x_{i,k+1}^A(0) - x_{i,k}^D(0) \right) \frac{x_T - x_{i,k}^D(t)}{x_{i,k+1}^A(t) - x_{i,k}^D(t)}, \tag{25}$$

$$x_{i,l}(0) = \begin{cases} x_{i,k}^D(0) + \left(x_{i,k+1}^A(0) - x_{i,k}^D(0) \right) \dfrac{x_T - x_{i,k}^D(t)}{x_{i,k+1}^A(t) - x_{i,k}^D(t) - w_i^{k,k+1}(t)}, & x_T < x_i^{k,k+1}(t), \\ \\ x_{i,k}^D(0) + \left(x_{i,k+1}^A(0) - x_{i,k}^D(0) \right) \dfrac{x_i^{k,k+1}(t) - x_{i,k}^D(t)}{x_{i,k+1}^A(t) - x_{i,k}^D(t) - w_i^{k,k+1}(t)}, & x_i^{k,k+1}(t) \leq x_T \leq x_i^{k,k+1}(t) + w_i^{k,k+1}(t), \\ \\ x_{i,k}^D(0) + \left(x_{i,k+1}^A(0) - x_{i,k}^D(0) \right) \dfrac{x_i^{k,k+1}(t) - x_{i,k}^D(t) - w_i^{k,k+1}(t)}{x_{i,k+1}^A(t) - x_{i,k}^D(t) - w_i^{k,k+1}(t)}, & x_T > x_i^{k,k+1}(t) + w_i^{k,k+1}(t). \end{cases} \tag{26}$$

4.3.2. Network Delay Characteristics. Taking the dispatching section *Nanjingnan–Hangzhoudong* as an example, the *ID* distributions of different trains under the rescheduled scheme can be figured out based on a coded calculation of equations (24)–(26) as indicated in Figure 18. The horizontal axis represents the natural time, the left vertical axis denotes the *ID* of each affected train, and the right vertical axis corresponds to the aggregate instantaneous delay of all affected trains. The dot lines stand for the *ID* variation of trans-in trains, and the initial delays of trans-in trains are determined by their rescheduled timetable in the upstream dispatching sections. The solid lines stand for the *ID* variation of other trains, including trans-in trains from other unaffected dispatching sections and trains starting operation from the current dispatching section. The thick blue line stands for the aggregate *ID* variation of all trains. The trans-in train delays start to fall to 0 after 13:00 because the trans-in trains are about to arrive at their destination successively. Under the conflict resolution strategies of train overtaking and buffer time utilization, the majority of other train delays fluctuate between 0 and 0.2 h (12 min).

Generally, the instantaneous delays of 9 trans-in trains from the *Xuzhoudong–Nanjingnan* dispatching section are apparently larger than the delays of other trains, and the initial trans-in delays are almost above 0.4 h, such as trains G1965, G19, G51, and G1889. As to the aggregate *ID* of all trains during the current time domain, it shows a relatively symmetrical rise-fall trend with a peak value of 6.23 h, where the fluctuant decrease arises from the comprehensive influences of train leaving, buffer utilization, and other train rescheduling.

Since *CD* targets at the station departure delays, it can be statistically analyzed by a larger interval, here taking the value of 5 min. Given the rescheduled and planned timetables of affected dispatching sections, the corresponding *CD*s can be obtained according to equation (23). Figure 19 shows the different variation curves, where the sum of *CD*s in different dispatching sections within the local network is defined as the network cumulative delay (*NCD*).

For the original dispatching section (*Xuzhoudong–Nanjingnan*), the *CD* growth rate increases first before 11:50 due to the rapid increase in affected trains and then decreases from 11:50 to 13:30 due to the reasonable resolution
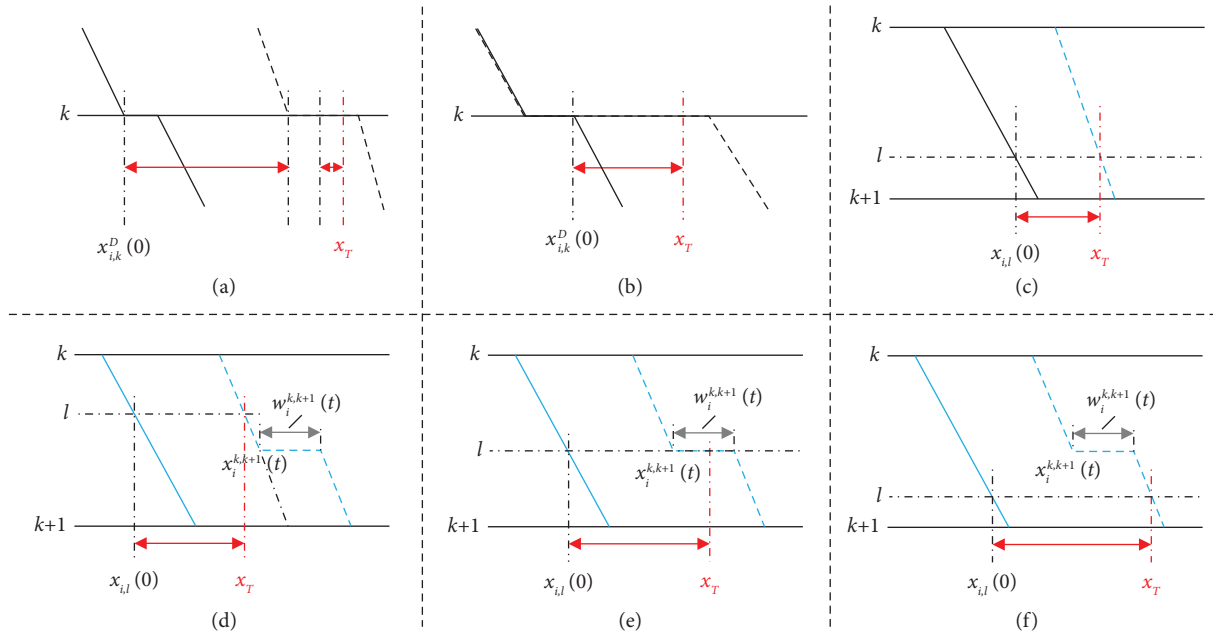
FIGURE 17: Instantaneous delay illustration under different scenarios. (a) Rescheduled arrival. (b) Rescheduled departure. (c) Without temporary stop. (d) Before temporary stop. (e) During temporary stop. (f) After temporary stop.
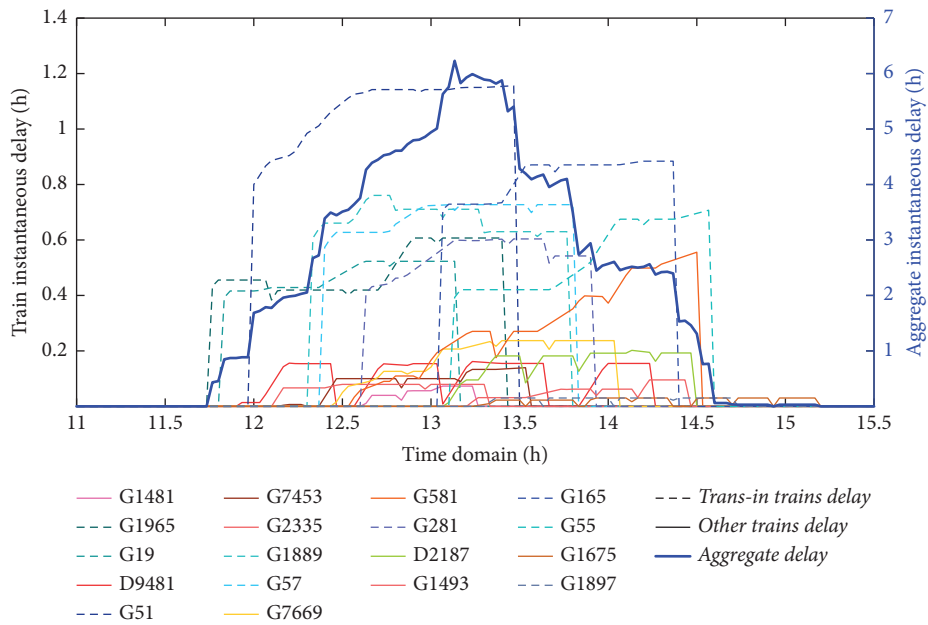

FIGURE 18: The ID variation of *Nanjingnan–Hangzhoudong* HSR under the rescheduled timetable.

of train conflicts and the efficient utilization of buffer times. After 13:30, almost every affected train has left the current dispatching section, and the *CD* remains constant. For the adjacent affected dispatching sections, the *CD* begins to generate at the time when the first affected trans-line train departs from the first station of the current dispatching section and takes on a linear growth trend before stabilization.

As for the *NCD*, the corresponding growth rate first increases and then decreases, where the inflection point appears at the time when the *CD* of the original dispatching section becomes stable. According to the *NCD* variation, the network delay propagation under current disturbance can be divided into the following four stages with different characteristics:
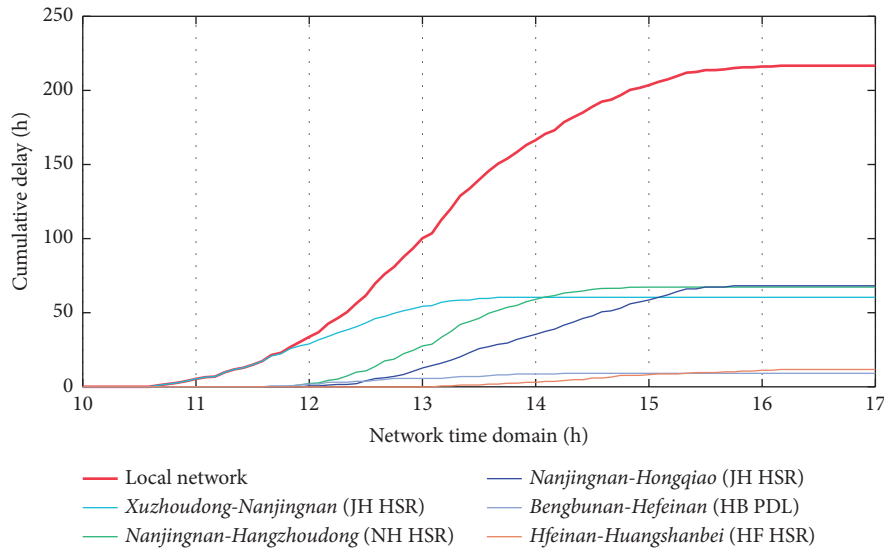
FIGURE 19: The CD variation curves of affected dispatching sections and local networks.

Stage 1: Slow growth stage (10:00~11:50). The *NCD* growth rate stays the same with the *CD* of the original dispatching section because the trans-line delay propagation has not formed.

Stage 2: Rapid growth stage (11:50~13:30). With trans-line operation of affected trains, train delay is propagating into the adjacent dispatching sections gradually, leading to varying degrees of secondary delay of other trains.

Stage 3: Growth slowdown stage (13:30~15:30). In this stage, the *CD* of the original dispatching section has stabilized, while the *CD*s of other adjacent-affected dispatching sections are still growing or beginning to stabilize.

Stage 4: Stabilization stage (15:30~17:00). The *CD* of every dispatching section has become steady, and the *NCD* enters the stable stage.

4.4. Algorithm Tests

4.4.1. Representative Scenario Tests. Since the core of the proposed method is coordinated conflict resolving and global rescheduling, additional cases have been tested to validate the effectiveness. Three representative scenarios have been tested, including a disturbance caused by station track malfunction on the Nanjing–Shanghai HSR, a disturbance caused by foreign object invasion on the Shanghai–Wuhan HSR, and a disturbance caused by EMU failure on the Hangzhou–Shenzhen HSR. The corresponding test results are indicated in Table 6. Comparing with the actual dispatching graph, the proposed method can efficiently reduce the aggregate train delay and the aggregate weighted

train delay, and the testing results show that the improvement rate will increase with the planned service frequency and the remaining running distance. Meanwhile, the average train adjustments of optimized schemes are slightly changed as compared to the adjustments under actual schemes, while the total number of train adjustments decreases to a different degree under the test scenarios because the number of affected trains gets reduced.

4.4.2. Computation Time Tests. The algorithmic process is a time-consuming procedure, especially in the conflict resolving module. The computation time distribution of different algorithm modules under different scenarios is indicated in Table 7. According to the test results, the computation time increases with the increasing primary delay, and disturbances occurring in sections consume more time than station disturbances. In the time distribution, algorithms of DFS pruning, strategy tree generation, and conflict resolution account for almost 70% of the total computation time, while algorithms of parameter extraction and Nash equilibrium consume similar computation time under different scenarios. For primary delays less than 25 min, the proposed method can output the rescheduled timetable in time, with the computation time less than the disturbance duration. However, for primary delays between 25 and 40 min, our proposed method would become more time-consuming, and the total computation time would exceed the primary delay, which means that it would be hard to output executable dispatch plans for affected trains during the disturbance duration time. The problem of time-consuming computation can be solved by more efficient coding and a higher-performance computer with faster CPUs and RAMs.

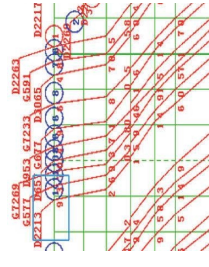TABLE 6: The test results of typical cases under different disturbances.

Scenarios	1		2		3	
Location	Nanjing–Shanghai HSR		Shanghai–Wuhan HSR		Hangzhou–Shenzhen HSR	
Disturbance	Section blockage with a primary delay of 22 min, caused by forward track malfunction		A primary departure delay of 14 min, caused by foreign object invasion		Temporary section blockage with a primary delay of 16 min, caused by EMU failure	
Indicator	Actual scheme	Optimized scheme	Actual scheme	Optimized scheme	Actual scheme	Optimized scheme
Affected trains	9	6	9	7	7	5
Aggregate delay (h)	4.37	2.87 (↓ 34.3%)	3.79	3.14 (↓ 17.1%)	2.75	2.52 (↓ 9.1%)
Aggregate weighted delay (h)	17.80	8.95 (↓ 49.7%)	12.11	9.94 (↓ 17.9%)	9.62	7.93 (↓17.6%)
Average adjustments	4.67	4.83 (↑ 3.4%)	3.89	3.71 (↓ 4.8%)	2.86	3.00 (↑ 4.9%)

TABLE 7: Average computation time of the proposed approach (unit: s).

Module	Algorithm	PD ≤ 10 min		10 < PD ≤ 25 min		25 < PD ≤ 40 min	
		Station	Section	Station	Section	Station	Section
Conflict resolving	Parameter extraction	5.6	5.9	5.8	5.7	5.6	5.8
	Conflict detection	42.4	47.1	64.1	68.2	99.3	114.6
	Conflict resolution	68.5	76.3	189.3	256.9	421.7	495.6
	Status update	12.3	13.7	11.9	14.5	13.2	15.2
	Strategy tree generation	111.1	123	291.3	387.2	647.2	760.1
Global optimizing	DFS pruning	145.2	171	420.1	552.8	988.6	1185.7
	Pareto optimization	11.3	11.6	24.3	26.5	31.2	35.3
	Nash equilibrium	2.9	2.8	2.9	2.9	3	3.1
Total		399.3	451.4	1009.7	1314.7	2209.8	2615.4

5. Conclusions and Future Research

As previously discussed, the major contributions of this paper lie in the following three aspects: The first contribution lies in the tree-based conflict resolving mechanism, considering the prior conflict and corresponding resolution strategies under different delay propagation scenarios with in-depth combination of spatiotemporal resources and technical operation rules. The second contribution is the biobjective programming model, where the objective of average train adjustments, the constraints of maximum train avoidance, and the affected train number are original, which can better balance the disturbance influence and dispatching robustness. Meanwhile, the model is solved by Pareto optimality and Nash equilibrium in order to guarantee global optimality. The third contribution is the integrated algorithm designing for network rescheduling considering the delay propagation effect within adjacent dispatching sections, together with two proposed indicators of cumulative delay and instantaneous delay, which can facilitate the real-time and off-line evaluation of delay propagation dynamics.

As to the limitations and challenges in real-world scenarios, the stochasticity of train speed control and the potential risk of other disturbances are the major challenges. Other factors, including the accuracy of the original data, the allocation of station track usage, and the uncertainty of facility or equipment status, would also affect the reliability of the results.

Future research will be focused on train platforming optimization under network delay propagation to realize a dynamic coordination between timetable adjustment and station track utilization. It would also be interesting to further consider the objectives and constraints from the perspective of train speed control, such as running comfortability and energy consumption, in order to achieve the integration of demand response, train rescheduling, and operation control. Nevertheless, the proposed rescheduling model and algorithm can effectively detect train conflicts and generate feasible timetables for train dispatching under recoverable disturbances.

Data Availability

The data supporting the current study are available from the corresponding author upon request.

Conflicts of Interest

The authors declare that there are no conflicts of interest regarding the publication of this paper.

Acknowledgments

References

[1] K. Akita, T. Watanabe, H. Nakamura, and I. Okumura, "Computerized interlocking system for railway signaling control: smile," *IEEE Transactions on Industry Applications*, vol. 21, no. 3, pp. 826–834, 1985.

[2] B. Szpigel, "Optimal train scheduling on a single track railway," *Operations Research*, vol. 72, pp. 344–351, 1973.

[3] M. Mazzarello and E. Ottaviani, "A traffic management system for real-time traffic optimisation in railways," *Transportation Research Part B: Methodological*, vol. 41, no. 2, pp. 246–274, 2007.

[4] A. Toletti, M. Laumanns, and U. Weidmann, "Coordinated railway traffic rescheduling with the Resource Conflict Graph model," *Journal of Rail Transport Planning and Management*, vol. 15, Article ID 100173, 2020.

[5] F. Corman, A. D'Ariano, D. Pacciarelli, and M. Pranzo, "Evaluation of green wave policy in real-time railway traffic management," *Transportation Research Part C: Emerging Technologies*, vol. 17, no. 6, pp. 607–616, 2009.

[6] S. Van Thielen, F. Corman, and P. Vansteenwegen, "Towards a conflict prevention strategy applicable for real-time railway traffic management," *Journal of Rail Transport Planning and Management*, vol. 11, Article ID 100139, 2019.

[7] S. Van Thielen, F. Corman, and P. Vansteenwegen, "Considering a dynamic impact zone for real-time railway traffic management," *Transportation Research Part B: Methodological*, vol. 111, pp. 39–59, 2018.

[8] S. Jiang, C. Persson, and J. Akesson, "Punctuality prediction: combined probability approach and random forest modelling with railway delay statistics in Sweden," in *Proceedings of the IEEE Intelligent Transportation Systems Conference (ITSC)*, Auckland, New Zealand, November 2019.

[9] B. Gao, D. Ou, D. Dong, and Y. Wu, "A Data-driven two-stage prediction model for train primary-delay recovery time," *International Journal of Software Engineering and Knowledge Engineering*, vol. 30, no. 07, pp. 921–940, 2020.

[10] N. Marković, S. Milinković, K. S. Tikhonov, and P. Schonfeld, "Analyzing passenger train arrival delays with support vector regression," *Transportation Research Part C: Emerging Technologies*, vol. 56, pp. 251–262, 2015.

[11] P. Huang, Q. Peng, C. Wen, and Z. Li, "Study on high-speed railway disruption classification and model of its influence on train number," *China Safety Science Journal*, vol. 28, no. S2, pp. 46–53, 2018.

[12] A. Thaduri, "Nowcast models for train delays based on the railway network status," *International Journal of System Assurance Engineering and Management*, vol. 11, no. S2, pp. 184–195, 2020.

[13] B. S. Grandhi, E. Chaniotakis, S. Thomann, F. Laube, and C. Antoniou, "An estimation framework to quantify railway disruption parameters," *IET Intelligent Transport Systems*, vol. 15, no. 10, pp. 1256–1268, 2021.

[14] R. M. P. Goverde, "Railway timetable stability analysis using max-plus system theory," *Transportation Research Part B: Methodological*, vol. 41, no. 2, pp. 179–201, 2007.

[15] R. M. P. Goverde and I. A. Hansen, "TNV-prepare: analysis of Dutch railway operations based on train detection data," *Computers in Railways VII*, C. A. Brebbia, Ed., WIT Press, Bologna, Italy, 2000.

[16] S. Harrod, F. Cerreto, and O. A. Nielsen, "A closed form railway line delay propagation model," *Transportation Research Part C: Emerging Technologies*, vol. 102, pp. 189–209, 2019.

[17] M. J. Dorfman and J. Medanic, "Scheduling trains on a railway network using a discrete event model of railway traffic," *Transportation Research Part B: Methodological*, vol. 38, no. 1, pp. 81–98, 2004.

[18] A. Mascis and D. Pacciarelli, "Job-shop scheduling with blocking and no-wait constraints," *European Journal of Operational Research*, vol. 143, no. 3, pp. 498–517, 2002.

[19] P. Wang, L. Ma, R. M. P. Goverde, and Q. Wang, "Rescheduling trains using Petri Nets and heuristic search," *IEEE Transactions on Intelligent Transportation Systems*, vol. 17, no. 3, pp. 726–735, 2016.

[20] Y. Zhang, Q. Zhong, Y. Yin, X. Yan, and Q. Peng, "A fast approach for reoptimization of railway train platforming in case of train delays," *Journal of Advanced Transportation*, vol. 2020, no. 4, Article ID 5609524, 20 pages, 2020.

[21] Y. Zhang, Z. Chen, M. An, and A. M. Umar, "An integration of train timetabling, platforming and routing-based cooperative adjustment methodology for dealing with train delay," *International Journal of Software Engineering and Knowledge Engineering*, vol. 30, no. 07, pp. 901–919, 2020.

[22] A. Caprara, L. Galli, S. Stiller, and P. Toth, "Delay-robust event scheduling," *Operations Research*, vol. 62, no. 2, pp. 274–283, 2014.

[23] Z. Feng, C. Cao, and Y. Liu, "Train delay propagation under random interference on high-speed rail network," *International Journal of Modern Physics C*, vol. 30, no. 08, Article ID 1950059, 2019.

[24] G. Filcek, D. Gsior, M. Hojda, and J. Józefczyk, "An algorithm for rescheduling of trains under planned track closures," *Applied Sciences*, vol. 11, no. 5, pp. 2334.1–41, 2021.

[25] C. Schön and E. König, "A Stochastic dynamic programming approach for delay management of a single train line," *European Journal of Operational Research*, vol. 271, no. 2, pp. 501–518, 2018.

[26] M. Samà, A. D'Ariano, F. Corman, and D. Pacciarelli, "A variable neighbourhood search for fast train scheduling and routing during disturbed railway traffic situations," *Computers and Operations Research*, vol. 78, pp. 480–499, 2017.

[27] K. Keita, P. Pellegrini, and J. Rodriguez, "A three-step Benders decomposition for the real-time railway traffic management problem," *Journal of Rail Transport Planning and Management*, vol. 13, Article ID 100170, 2020.

[28] S. P. Josyula, J. Törnquist Krasemann, and L. Lundberg, "A parallel algorithm for train rescheduling," *Transportation Research Part C: Emerging Technologies*, vol. 95, pp. 545–569, 2018.

[29] X. Zhou, Q. Zhang, W. Xu, T. Wang, and P. Song, "Intelligent adjustment method for train operation diagram with consideration of motor train set connection," *Journal of the China Railway Society*, vol. 40, no. 8, pp. 19–27, 2018.

[30] G. Cavone, V. Montaruli, T. J. J. van den Boom, and M. Dotoli, "Demand-oriented rescheduling of railway traffic in case of delays," in *Proceedings of the 2020 7th International Conference on Control, Decision and Information Technologies (CoDIT)*, Prague, Czech Republic, June 2020.

[31] P. Wang and R. M. P. Goverde, "Multi-train trajectory optimization for energy efficiency and delay recovery on single-track railway lines," *Transportation Research Part B: Methodological*, vol. 105, pp. 340–361, 2017.

[32] F. Liu, J. Xun, R. Liu, J. Yin, and H. Dong, "A real-time rescheduling approach using loop iteration for high-speed railway traffic," *IEEE Intelligent Transportation Systems Magazine*, vol. 15, no. 1, pp. 318–332, 2023.

[33] I. Louwerse and D. Huisman, "Adjusting a railway timetable in case of partial or complete blockades," *European Journal of Operational Research*, vol. 235, no. 3, pp. 583–593, 2014.

[34] M. Schachtebeck and A. Schöbel, "To wait or not to wait-and who goes first? Delay management with priority decisions," *Transportation Science*, vol. 44, no. 3, pp. 307–321, 2010.

[35] Y. Zhu and R. M. P. Goverde, "Railway timetable rescheduling with flexible stopping and flexible short-turning during disruptions," *Transportation Research Part B: Methodological*, vol. 123, pp. 149–181, 2019.

[36] X. Li, Z. Yan, and B. Han, "An optimization adjustment method for delayed high-speed trains based on Multi-tree," *Journal of Transportation Systems Engineering and Information Technology*, vol. 19, no. 2, pp. 130–136, 2019.

[37] Y. Ye and J. Zhang, "Accident-oriented delay propagation in high-speed railway network," *Journal of Transportation Engineering, Part A: Systems*, vol. 146, no. 4, 2020.

[38] M. Shakibayifar, A. Sheikholeslami, and A. Jamili, "A multi-objective decision support system for real-time train rescheduling," *IEEE Intelligent Transportation Systems Magazine*, vol. 10, no. 3, pp. 94–109, 2018.